

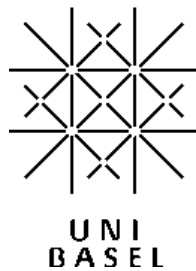
Master Thesis  
Summer Semester 2007

---

# Multi-particle qubits

---

Oded Zilberberg  
Department of Physics and Astronomy



Supervision by Prof. Dr. Daniel Loss

## Contents

<b>1</b>	<b>Introduction</b>	<b>5</b>
<b>2</b>	<b>Introduction to quantum computation</b>	<b>7</b>
2.1	Quantum computer architecture . . . . .	7
2.2	Quantum bit (qubit) . . . . .	7
2.3	Measurement . . . . .	8
2.4	Multiple qubits . . . . .	8
2.5	Quantum gates . . . . .	9
2.6	Universal set of gates . . . . .	10
<b>3</b>	<b>Multi-spin qubits - setting the stage</b>	<b>11</b>
3.1	Qubit encoding schemes of physical systems . . . . .	11
3.1.1	Projection on a two-level system . . . . .	12
3.1.2	Partial projection . . . . .	13
3.1.3	No projection . . . . .	13
3.2	Multi-spin qubit gates . . . . .	13
3.2.1	Spin-“braiding” . . . . .	14
3.3	Physical systems . . . . .	17
3.3.1	Electron spin in quantum dots . . . . .	17
3.3.2	Photon in a cavity . . . . .	18
3.3.3	Schwinger bosons . . . . .	18
<b>4</b>	<b>The quest for anyon statistics</b>	<b>20</b>
4.1	Anyon statistics are not reproducible (a “false quest”) . . . . .	20
4.1.1	A non-Abelian spin-braiding scheme . . . . .	21
4.1.2	Braiding spins cannot mimic Ising-anyon braiding statistics	22

CONTENTS

---

4.1.3	Summary	25
4.2	Spin permutations as qubit rotations and two-qubit entanglement	26
4.2.1	Single qubit rotation	26
4.2.2	two-qubit entanglement	27
4.2.3	Summary	29
4.3	The properties of a non-linear computational mapping	30
4.3.1	Operations	33
4.3.2	Computational division by operator eigenstates	35
4.3.3	Conclusions	35
4.4	Summary	36
<b>5</b>	<b>CNOT on a singlet-triplet basis</b>	<b>38</b>
5.1	A classical CNOT	39
5.1.1	Spin-braiding between the qubits	40
5.1.2	Projection back to the computational space	40
5.1.3	A classical CNOT can be obtained	43
5.1.4	Summary	43
5.2	CNOT using spin parity measurements	44
5.2.1	Equivalence between spin parity and singlet-triplet parity	44
5.2.2	The CNOT gate	46
5.2.3	Summary	48
5.3	Summary	49
<b>6</b>	<b>Summary</b>	<b>50</b>
6.1	Overview	50
6.2	Outlook	50

*CONTENTS*

---

<b>7 Acknowledgments</b>	<b>52</b>
<b>A Singlet-triplet parity encoder</b>	<b>53</b>
<b>B Verification of the CNOT gate operation</b>	<b>54</b>
B.1 Proof over pure computational basis states . . . . .	54
B.2 Proof of linearity . . . . .	56

## 1 Introduction

The topic of *Quantum Computation* was born out of the two scientific fields of *Physics* and *Computer Science*. Computer Science is a mathematical-theoretical field but its implementation has always been physical. A computer is constructed from physical materials, e.g. Silicon transistors, for which deep understanding of the principles of Physics and material science is required.

Since the invention of the transistor, computer hardware has grown in power at an amazing pace - double the computer power for constant cost every 18 months. This growth rate has been named *Moore's law* and served as a guideline for computer industry aspiration. However, an end to Moore's law growth rate is expected, as fabrication techniques are reaching a size regime where quantum effects play a greater role. A possible solution to this problem is to implement the computers of the future with quantum systems.

Computation with quantum systems, i.e. quantum computation, is different in essence from classical computation (see Chapter 2). It has been proven that a quantum computer will be a more powerful computing machine [1]. Thus, a quantum computer gives hope that Moore's law can be maintained and opens up new computing directions and algorithms that are not feasible on a classical computer.

Several physical systems have been suggested as possible candidates for the implementation of a quantum computer:

- Electron spins in quantum dots
- Superconducting qubits
- Ions in magnetic traps
- Spins in large molecules using Nuclear Magnetic Resonance (NMR)
- Atoms in optical lattices
- Non-Abelian anyons

Research goes on, in attempt to find other physical alternatives and explore the possibilities of constructing a functional quantum computer.

In this thesis we discuss a scheme in which the quantum computer’s logical unit (the qubit) is implemented by a system composed of several elementary particles. We call this system a *multi-particle qubit*. Several such schemes have already been proposed, e.g. qubits encoded by varying number of spin-1/2 particles [2, 3, 4, 5, 6, 7, 8] and qubits encoded by multiple “Ising-type” anyons [9]. Our qubits are also composed of multiple spin-1/2 particles.

We discuss several approaches for implementation of quantum computation over multiple spin-1/2 qubits. We divide the ways of encoding a qubit into three categories and introduce each category using case studies. For each qubit encoding scheme we search for possible physical operations that will implement universal quantum computation over this qubit and, thus, pose a suitable candidate for a quantum computer architecture.

We find that two of the encoding categories, which are less commonly researched, are difficult to realize and we explain the problems in such approaches alongside a general overview of multi-particles qubits properties. The third encoding category of complete projection on a two-level system, is the most commonly used approach. In our study of this encoding scheme type we present a specific system of singlet-triplet qubits. For the singlet-triplet qubits we implement a Controlled-NOT (CNOT) gate which is an important element in universal quantum computation.

In Chapter 2 we introduce the basic concepts of quantum computation and establish a common language. Chapter 3 sets the stage for the multi-particle qubit scheme. In Chapter 4 we map the difficulties of implementing a universal quantum computer over such a multi-particle qubit using a given set of physical particle-exchange operations. In Chapter 5 we implement a CNOT gate on a two-spin singlet-triplet qubit using spin parity measurements.

## 2 Introduction to quantum computation

Quantum physics has been studied for over a hundred years. Applying its ideas to the construction of a quantum computer has introduced a new field of research - “*Quantum Computation*”. In this chapter we summarize the main concepts of this field in order to establish a common language.

### 2.1 Quantum computer architecture

We define a classical computer as a device which operates on bits (binary arithmetic). The device computes by manipulating those bits, i.e. by transporting these bits from memory to logic gates and back.

A quantum computer, in contrast, operates on a set of qubits (quantum bits). It computes by manipulating those qubits, i.e. by transporting these qubits from memory to quantum logic gates and back.

### 2.2 Quantum bit (qubit)

A classical bit is a physical implementation of *Binary Arithmetic Digits*. It can be in two states 0/1.

Quantum bits (qubits) are a physical implementation of a quantum two-level system. Such a system is described by a two-dimensional Hilbert space  $\mathcal{H}_2^{comp.}$  that is spanned by the basis states  $|0\rangle/|1\rangle$  (i.e.  $\mathcal{H}_2^{comp.} = span\{|0\rangle, |1\rangle\}$ ).

A general state of a qubit (a general superposition of basis states) is:

$$|\psi\rangle = \alpha |0\rangle + \beta |1\rangle, \quad (2.1)$$

where  $|\psi\rangle$  is generally assumed to be normalized, i.e.  $|\alpha|^2 + |\beta|^2 = 1$  and  $\alpha, \beta \in \mathbb{C}$ .

From Eq. (2.1) it is easy to deduce (see Ref. [1]) a useful geometric representation of qubits as points on a unit sphere in three-dimensional space (i.e. *Bloch sphere*) see Fig. 1.

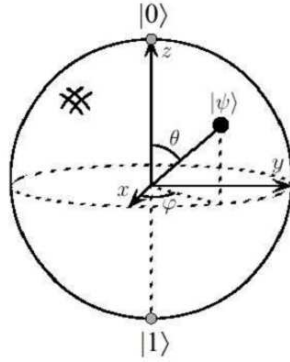


Figure 1: Bloch sphere - A unit sphere in three-dimensional space. The pure basis states lie on the two poles. A point on the sphere is defined by two angles:  $\theta$  and  $\phi$  and is equivalent to a specific superposition of the basis states  $|0\rangle$  and  $|1\rangle$ .

### 2.3 Measurement

Measuring a classical bit returns its state 0/1 (READ operation).

Measuring a qubit forces the qubit's state into one of the two basis states  $|0\rangle / |1\rangle$ . The outcome of a measurement is probabilistic and depends on the original qubit state:

$$\hat{M} |\psi\rangle = \begin{cases} |0\rangle & \text{with probability } |\alpha|^2, \\ |1\rangle & \text{with probability } |\beta|^2. \end{cases} \quad (2.2)$$

Repeated measurements of the qubit will return the same state with probability 1, as the state has changed by the measurement and is well-defined.

### 2.4 Multiple qubits

Until now we have discussed the properties of a 1-qubit system. A system of  $N$ -qubits is described by a tensor product space of  $N$  two-dimensional Hilbert spaces  $\mathcal{H}_n = \mathcal{H}_2 \otimes \dots \otimes \mathcal{H}_2$  (where  $n = 2^N$ ) that is spanned by the basis states  $|0\dots 00\rangle, |0\dots 01\rangle, |0\dots 10\rangle, \dots, |1\dots 11\rangle$ .

As an example for an  $N$ -qubit system let us consider  $N = 2$ . The general state would be an arbitrary normalized superposition of basis states:

$$|\psi\rangle_2 = \alpha_{00} |00\rangle + \alpha_{01} |01\rangle + \alpha_{10} |10\rangle + \alpha_{11} |11\rangle \quad (2.3)$$

The probability of measuring both qubits in a specific state  $|ab\rangle$  (where  $a, b \in \{0, 1\}$ ) is once more the square of the amplitudes ( $\hat{M}|\psi\rangle_2 = |ab\rangle$  with probability  $|\alpha_{ab}|^2$ ). An *entangled* state is a state in which a measurement of one of the qubits will affect the other qubit's state as well. If the qubits are not *entangled* the measurement of one of the bits does not affect the other and thus the probability (for example) to measure the 1st qubit in state  $|0\rangle$ , i.e.  $\hat{M}_1|\psi\rangle_2 = |0b\rangle$ , is  $|\alpha_{00}|^2 + |\alpha_{01}|^2$ .

An example of a completely entangled state is given by:

$$\frac{|00\rangle + |11\rangle}{\sqrt{2}}. \quad (2.4)$$

A measurement of the first qubit results in state  $|0\rangle$  or state  $|1\rangle$  with probability 0.5. After the first qubit is measured, for example in state  $|0\rangle$ , a measurement of the second qubit will always find it in state  $|0\rangle$ .

## 2.5 Quantum gates

A quantum gate is the quantum analogy to classical computer gates. Such a quantum gate receives input qubits and outputs altered output qubits. From the postulates of quantum mechanics, such a gate must be a linear unitary operation. We present the group of single-qubit gates in order to illustrate this condition.

Single-qubit gates have one input qubit and one output qubit. The group of all linear unitary operations over a single qubit (i.e. two dimensional Hilbert space) is equivalent to a  $SU(2)$  algebra. A useful representation of such an algebra is provided by  $2 \times 2$  matrices operating on the computational basis states  $|0\rangle, |1\rangle$ . We present here some important single qubit gates that we will use during this thesis:

$$\hat{\sigma}_x \equiv \begin{bmatrix} 0 & 1 \\ 1 & 0 \end{bmatrix} \quad \hat{\sigma}_z \equiv \begin{bmatrix} 1 & 0 \\ 0 & -1 \end{bmatrix} \quad \hat{H} \equiv \frac{1}{\sqrt{2}} \begin{bmatrix} 1 & 1 \\ 1 & -1 \end{bmatrix}. \quad (2.5)$$

The  $SU(2)$  algebra corresponds to rotations of the qubit's state on the Bloch sphere. As an example we present the Hadamard gate  $\hat{H}$  on the Bloch sphere (see Fig. 2).

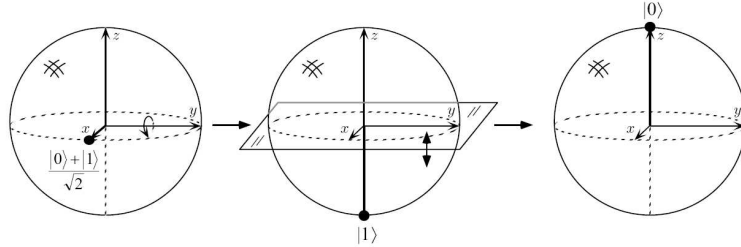


Figure 2: Hadamard gate visualization on a Bloch sphere - A turn by  $90^\circ$  counter clockwise around the  $y$  axis, followed by a reflection on the  $xy$ -plane yields the Hadamard gate's operation. In  $SU(2)$ , reflections and rotations can be translated to rotations around an arbitrary axis. Thus, the Hadamard operation is equivalent to a rotation on the Bloch sphere.

## 2.6 Universal set of gates

A set of gates is said to be *universal* if it alone can replicate the effects of all other gates needed for computation.

It turns out (a proof can be found in Ref. [1]) that a universal quantum set of gates exists. It is sufficient (for example) to take the set of all single-qubit rotations ( $SU(2)^{\otimes N}$ ) together with the two-qubit CNOT gate. Such a set is composed of *local qubit operations* that affect only one qubit at a time and an entangler of two qubits (*non-local qubit operation*).

Other such sets of universal gates exist. They all contain a representative non-local gate as it is the only way to implement entanglement of qubits. In this thesis we try to implement the following universal set on our multi-particle qubits:

$$G = \underbrace{\{\hat{\sigma}_x, \hat{\sigma}_y, \hat{\sigma}_z, e^{i\frac{\pi}{4}\hat{\sigma}_z}\}}_{\text{single qubit gates}}, \underbrace{\{e^{i\frac{\pi}{4}\hat{\sigma}_x \times \hat{\sigma}_x}\}}_{\text{two-qubit gate}}. \quad (2.6)$$

Thereafter, we implement a CNOT gate on a pair of singlet-triplet qubits, and show another scheme for universal quantum computation on that system.

### 3 Multi-spin qubits - setting the stage

In this chapter we set the stage for our work on multi-spin qubits. We introduce the main questions that arise when dealing with such a system.

#### 3.1 Qubit encoding schemes of physical systems

Qubits are the computational encoding of a quantum two-level system. Each quantum level is given a specific logical value in order to understand the computation performed over these physical states. One such two-level system is the electron spin 1/2. In order to use it as a qubit we linearly map its pure spin states into quantum logical states

$$f(|\psi\rangle) := \begin{cases} |0\rangle & \text{if } |\psi\rangle = |\uparrow\rangle, \\ |1\rangle & \text{if } |\psi\rangle = |\downarrow\rangle. \end{cases} \quad (3.1)$$

We call  $f$  a “computational mapping” function. It defines the way a qubit is encoded over a given physical system. Using this function, we can formalize our claims about different qubit encoding schemes. We discuss the properties of different computational mappings throughout this thesis.

We note that over the spin 1/2 system, the computational mapping is a homomorphism between the two-dimensional spin Hilbert space and the two-dimensional qubit Hilbert space:

$$f : \mathcal{H}_2 \rightarrow \mathcal{H}_2^{comp.} \quad (3.2)$$

However, there are other physical systems which are not two-level systems but can be mapped onto a two dimensional Hilbert space which, in turn, might be used for quantum computation. Among such systems are multi-spin qubits. These are systems composed of  $N$  non-interacting spins 1/2. Their general state  $|\psi\rangle_N \in \mathcal{H}_n$  (where  $n = 2^N$  and  $|\psi\rangle_N$  is normalized) can be decomposed into the multi-spin normal basis

$$|\psi\rangle_N = \sum_{\sigma_1, \dots, \sigma_N = \uparrow, \downarrow} \alpha_{\sigma_1, \dots, \sigma_N} |\sigma_1 \dots \sigma_N\rangle, \quad (3.3)$$

and the computational mapping will be the non-linear function<sup>1</sup>:

$$f : \mathcal{H}_n \rightarrow \mathcal{H}_2^{comp.} \quad (3.4)$$

---

<sup>1</sup>An m-qubit interpretation we are looking for a mapping  $\tilde{f} = f \times f \times \dots \times f : \mathcal{H}_{n^m} \rightarrow \mathcal{H}_{2^m}^{comp.}$

One can divide the non-linear computational mappings into three main categories: Projection on a two-level system (see Section 3.1.1), partial projection (see Section 3.1.2), and no projection at all (see Section 3.1.3). Projection on a two-level system is the most commonly used qubit encoding scheme. This is mainly because the other two categories are of mappings which are not *one-to-one* over their image<sup>2</sup> and hence, are more complicated.

The properties of these non-linear mappings are discussed thoroughly in this thesis (see Section 4.3). As for now, though, we just introduce the three categories. In order to do so, we will look at the case of a two-spin qubit ( $N = 2$ ). Here, the qubit is composed of two spins  $1/2$  and the computational mapping is the non-linear function  $f : \mathcal{H}_4 \rightarrow \mathcal{H}_2^{comp}$ .

### 3.1.1 Projection on a two-level system

The first option in mapping a higher-dimensional Hilbert space onto a two dimensional Hilbert space is to project all except two of the degrees of freedom out of the computational space (to the kernel<sup>3</sup> of the mapping). In the case of a two-spin qubit  $f$  sends two degrees of freedom to zero computational meaning. Over the remaining two basis states, it maps linearly into computational logical states. In Eq. (3.5) we see an example of such a mapping that defines a singlet-triplet qubit:

$$f(|\psi\rangle_2) := \begin{cases} 0 & \text{if } |\psi\rangle_2 \in \ker(f) = \text{span}\{|\uparrow\uparrow\rangle, |\downarrow\downarrow\rangle\}, \\ |0\rangle & \text{if } |\psi\rangle_2 = |T\rangle = \frac{|\uparrow\downarrow\rangle + |\downarrow\uparrow\rangle}{\sqrt{2}}, \\ |1\rangle & \text{if } |\psi\rangle_2 = |S\rangle = \frac{|\uparrow\downarrow\rangle - |\downarrow\uparrow\rangle}{\sqrt{2}}. \end{cases} \quad (3.5)$$

As long as the system is coherent and stays within the computational subspace, this two-level system can be used as a qubit. Such a projected subspace as in Eq. (3.5) can be physically engineered by choosing the states of aligned spins to be energetically unfavorable. However, operations exist that cause our physical system to step out of the computational space, e.g. a spin flip of one of the spins or spin exchange between qubits, which serve as a possible source of quantum information leakage, i.e. decoherence.

We discuss computational mappings from this category in Chapter 5 and Section 4.1.2.

---

<sup>2</sup>The *image* of a function  $f : X \rightarrow Y$  is defined as all the members  $y = f(x)$  such that  $y \in Y, x \in X$ , and  $y \neq 0$ , i.e.  $Im(f) = \{f(x) = y \in Y \mid x \in X, y \neq 0\}$ .

<sup>3</sup>The *kernel* of a function  $f : X \rightarrow Y$  is defined as all the members  $x \in X$  such that  $f(x) = 0$ , i.e.  $\ker(f) = \{x \in X \mid f(x) = 0\}$ .

### 3.1.2 Partial projection

In the “partial projection” case, some degrees of freedom are projected out of the computational space, i.e. the kernel of the computational mapping has a dimension larger than zero. The remaining states are divided into two computational sub-blocks. For the  $N = 2$  case, a possible mapping is the following:

$$f(|\psi\rangle_2) := \begin{cases} 0 & \text{if } |\psi\rangle_2 \in \ker(f) = \text{span}\{|\uparrow\uparrow\rangle\}, \\ \alpha|0\rangle & \text{if } |\psi\rangle_2 \in \text{span}\{|\uparrow\downarrow\rangle, |\downarrow\downarrow\rangle\}, \\ |1\rangle & \text{if } |\psi\rangle_2 = |\uparrow\downarrow\rangle. \end{cases} \quad (3.6)$$

where  $|\alpha|^2 = 1$  and  $\alpha \in \mathbb{C}$ .

Computational mappings from this category are *non-linear* over the image of the mapping. Their properties are discussed in Section 4.3, while, another example of such a mapping is shown in Section 4.2.

### 3.1.3 No projection

Finally, we look at the case where there is no projection at all. No degrees of freedom are projected out of the computational space. The set of states is divided into two computational sub-blocks. For the  $N = 2$  case, an example of such a mapping is:

$$f(|\psi\rangle_2) := \begin{cases} \alpha|0\rangle & \text{if } |\psi\rangle_2 \in \text{span}\{|\uparrow\uparrow\rangle, |\downarrow\downarrow\rangle, |\uparrow\downarrow\rangle + |\downarrow\uparrow\rangle\}, \\ |1\rangle & \text{if } |\psi\rangle_2 = |S\rangle = \frac{|\uparrow\downarrow\rangle - |\downarrow\uparrow\rangle}{\sqrt{2}}. \end{cases} \quad (3.7)$$

where  $|\alpha|^2 = 1$  and  $\alpha \in \mathbb{C}$ .

Such mappings are also *non-linear* over the image of the mapping. In this thesis, we present the difficulties in finding such mappings that will enable quantum computation (see Section 4.3).

## 3.2 Multi-spin qubit gates

There are infinitely many computational mappings (results from the infinite cardinality of Hilbert space). However, in order to perform quantum computation on some multi-spin qubits, we must find physical operators that construct a universal set of quantum gates under a given qubit encoding.

In other words, let  $G$  be a universal set of quantum gates, and  $B$  be a group of physical operators that act on  $N$ -spins. The primary constraint that the computational mapping  $f$  must fulfill is:

$$\forall \hat{g} \in G \exists \hat{b} \in B \quad \hat{g}f(|\psi\rangle_N) \equiv f(\hat{b}|\psi\rangle_N). \quad (3.8)$$

Thus, over a multi-spin qubit system we can perform universal quantum computation, if for all the computational gates needed for universal quantum computing  $G$ , we find physical operations  $B$  that are equal under the qubit mapping  $f$ . Therefore, we are searching for possible physical operations on an  $n$ -dimensional Hilbert space ( $\mathcal{H}_n$  where  $n = 2^N$ ). These physical operations  $B$  can be written as quantum mechanical operators that must be unitary ( $B \subset SU(n)$ ). From this, we can deduce that the computational mapping implies another non-linear mapping  $\tilde{f}$  between operator groups<sup>4</sup>:

$$\tilde{f} : B \subset SU(n) \rightarrow G \subset SU(2). \quad (3.9)$$

### 3.2.1 Spin-“braiding”

In search for the physical operations on a multi-spin qubit system that can be used to satisfy the constraint in Eq. (3.8), we draw inspiration from *topological quantum computation* (TQC).

In Ref. [9] a multi-anyon qubit is constructed. On it, Eq. (3.8) is satisfied using, among other operations, braiding of the anyon building blocks (for explanation of *braiding* see below). Following this, we try to form some sort of spin-“braiding” that will enable us to implement a universal set of gates on multi-spin qubits (see Chapter 4).

Such spin braiding operators are composed of operations that exchange the position of the spins (swap gates) plus single-spin rotations. This is a favorable scheme as these are local operators that might induce (as in Ref. [9]) non-local operations between the qubits, i.e. exchanging spins between two qubits might cause entanglement that is equivalent to a universal two-qubit gate.

In order to construct such spin braiding, we must first introduce the differences between anyon and spin exchange statistics:

#### Exchange statistics

The fundamental “elementary” particles exist in three spatial dimensions,

---

<sup>4</sup>For  $m$ -qubit operations the mapping is  $\tilde{f} = B \subset SU(n^m) \rightarrow G \subset SU(2^m)$

and thus all have either bosonic or fermionic integer exchange statistics. However, in two spatial dimensions the laws of physics allow for the existence of particles with fractional statistics [10, 11, 12]. This is so because in  $2D$  a closed loop executed by a particle around another particle is topologically distinct from a loop which encloses no particles, unlike the three-dimensional case. An exchange of two particles is equivalent to one particle executing half a loop around the other, so that a closed loop is equivalent to exchange squared.

The particles are said to have statistics  $\phi$  if, upon exchange, the two-particle wave function acquires a phase factor of  $\exp(i\pi\phi)$ . The integer statistics  $\phi_B = 2j$  and  $\phi_F = 2j + 1$ , where  $j = 0, \pm 1, \pm 2, \dots$  describe the familiar boson and fermion exchange statistics:  $\exp(i\pi\phi_B) = +1$  and  $\exp(i\pi\phi_F) = -1$ , respectively. Fractional statistics describe  $2D$  quasi-particles which are called *anyons*.

These quasi-particles are essentially some spatially localized elementary excitations of the  $2D$  many-body system. Their name originated from the word *any* [13], representing the arbitrary fractional exchange statistics of these quasi-particles.

The  $2D$  anyons are used in the *topological quantum computation* (TQC) scheme [14, 15, 16]. For the purposes of TQC a specific type of anyon is needed that has non-Abelian exchange statistics. These *non-Abelian anyons* have statistics depending on the orientation of their exchange (clockwise or counter-clockwise) described by nontrivial representations of the braid group. Thus, the exchange operation of non-Abelian anyons is dubbed *braid-ing*.

### Topological Quantum Computation

A computation in TQC is carried out by creating pairs of non-Abelian anyons from the ground state, separating them far apart, transporting individual anyons adiabatically around each other, and finally measuring the pairs of anyons together in a process named *fusion*.

A physical system that may serve as a platform for TQC is a two-dimensional electron gas in the fractional quantum Hall effect (FQHE) regime. The FQHE plateau at the filling fraction  $\nu = 5/2$  was observed by Willett et al. [17] in the late 1980s. Shortly thereafter Moore and Read [18] developed a theory predicting that elementary excitations of the  $\nu = 5/2$  state are non-Abelian anyons. The corresponding braid group representation was found by Nayak and Wilczek [19]. For the sake of brevity we shall refer to the anyons

existing in the  $\nu = 5/2$  state as *Ising anyons* (their exchange statistics can be described by monodromy of holomorphic correlation functions of the 2D Ising model [18]).

A pair of such “Ising-type” anyons can be interpreted as a fermion 2 level system and thus as a qubit. The result of their fusion is the classical outcome of the computation.

### Swap gate examples

At a first glance, we are encouraged to implement quantum gates on multi-spin qubits using spin-braiding. There are several simple naive examples of computational mappings for a two-spin qubit, on which some quantum gates can be implemented using spin swap only. We present here two such examples:

- **Degenerate singlet-triplet system** The computational mapping  $f$  does not project any degrees of freedom to the computational zero. The group of physical operators at our disposal,  $B$ , is composed of a simple swap of the two spins:

$$f(|\psi\rangle_2) := \begin{cases} |0\rangle & \text{if } |\psi\rangle_2 = |S\rangle = \frac{|\uparrow\downarrow\rangle - |\downarrow\uparrow\rangle}{\sqrt{2}}, \\ \alpha |1\rangle & \text{if } |\psi\rangle_2 \in \text{span}\{|\uparrow\uparrow\rangle, |\downarrow\downarrow\rangle, |\uparrow\downarrow\rangle + |\downarrow\uparrow\rangle\}. \end{cases} \quad (3.10)$$

where  $|\alpha|^2 = 1$  and  $\alpha \in \mathbb{C}$ ,

$$B = \{B_1\}.$$

Here,  $B_1$  is the swap between the two spins position.

Under this computational mapping, the exchange of the positions of the spins is the computational  $\sigma_z$  operation, i.e.  $f(B_1|\psi\rangle_2) = \sigma_z f(|\psi\rangle_2)$ . Note that spin exchange has fermionic statistics  $-1$ , which gives rise to this result.

- **Computational subspace** The computational mapping  $f$  projects the 4-level system to a two-level subspace. Over the remaining subspace it is a linear mapping that maps the two basis states to computational states:

$$f(|\psi\rangle_2) := \begin{cases} 0 & \text{if } |\psi\rangle_2 \in \ker(f) = \text{span}\{|\uparrow\uparrow\rangle, |\downarrow\downarrow\rangle\}, \\ |0\rangle & \text{if } |\psi\rangle_2 = |\downarrow\uparrow\rangle, \\ |1\rangle & \text{if } |\psi\rangle_2 = |\uparrow\downarrow\rangle. \end{cases} \quad (3.11)$$

$$B = \{B_1\} \quad \text{same as before.}$$

Under this projective computational mapping, the exchange of the positions of the spins is a  $\sigma_x$  operation, i.e.  $f(B_1 |\psi\rangle_2) = \sigma_x f(|\psi\rangle_2)$ .

In this case we ignored the fermionic statistics. The reasons for ignoring it are explained in Section 3.3.

Now that we have seen that quantum gates can be implemented over multi-spin qubits using only simple spin swap operations, we are encouraged in our search for a multi-spin system over which we can perform universal quantum computation. We increase the size of the physical system and introduce spin-braiding instead of simple spin swap. Thus, we add degrees of freedom to the choice of computational mappings and physical operations. Therefore, we might be able to implement a universal set of gates (see Chapter 4).

### 3.3 Physical systems

We have chosen to construct our pseudo-particle with free-electron spins. However, our research is mainly mathematical in the sense that we only address the spins as building blocks that can exchange places, while each building block forms a two-level quantum system by itself. Additionally, we ignored the overall phase of the anti-symmetry of fermionic statistics in some of the above examples. Hence, we could also use other physical two-level systems as our building blocks. In this section, we present several such systems and use this chance to justify our mathematical approach by presenting the existing underlying physical operations.

#### 3.3.1 Electron spin in quantum dots

An electron spin trapped in a quantum dot has been proposed by Loss and DiVincenzo [20] as a promising two-level system for implementing a qubit. Initialization, manipulation, and readout of the electron spin have already been demonstrated in this setup [21, 22] and proposals exist for multi-spin qubit implementation using this system [2, 3, 4, 5, 6, 7, 8]. However, these proposals, all rely on controlling the two-electron exchange interaction.

In our scheme, control over the two-electron exchange interaction is not necessary. The exchange of spin location can be achieved by using an empty

transit quantum dot onto which an electron will hop, leaving a vacancy into which the other electron can tunnel.

Another way to achieve spin swapping is by using the SWAP operation that was implemented in Ref. [21], but that would require control of the electron exchange interaction between all the quantum dots.

In either way, spin-braiding and multi-spin qubit encoding are physically feasible in this system.

### 3.3.2 Photon in a cavity

Manipulation of photons and measurement of photons in a cavity are a part of non-linear quantum optics research [23, 24, 25]. The goal of this research is to implement a qubit composed of photons. Although the photon has spin-1 it cannot align on the magnetic neutral state and thus forms a two-level system. This system can be used in a similar way to the quantum dot scheme. By exchanging the location of the photons the same effects on the multi-photon qubit will be achieved as we ignore the global exchange phase of bosons/fermions.

### 3.3.3 Schwinger bosons

A system of a photon in one of two cavities  $L, R$  is an optional two-level system that can serve as our qubit. The photon has an equal probability of being in either of the cavities and can be written as a Schwinger boson system:

Let  $a_i^\dagger$  and  $a_i$  be the creation and annihilation operators of a photon on the left ( $i = L$ ) or the right ( $i = R$ ) cavity.

The set of operators

$$S_+ = a_L^\dagger a_R, \quad S_- = a_R^\dagger a_L, \quad S_z = \frac{1}{2} (a_L^\dagger a_L - a_R^\dagger a_R) \quad (3.12)$$

form an  $SU(2)$  algebra and this system defines a two-level quantum system over which the computational mapping is a homomorphism:

$$f(|\psi\rangle) := \begin{cases} |0\rangle & \text{if the photon is in the left cavity,} \\ |1\rangle & \text{if the photon is in the right cavity.} \end{cases} \quad (3.13)$$

The Schwinger boson system, as presented in the above computational mapping, is a possible implementation scheme.

In order to use this system for the multi-particle qubits, the qubits are composed of the whole set of photon plus two cavities as building blocks. Thus, when we refer to a two-spin qubit system, the analogous Schwinger boson system is composed of four cavities and two photons.

It is important to note that in this scheme the photon cannot leave its designated two cavities without having a photon replace it. The braiding must result in a system that keeps the Schwinger boson structure, otherwise our mathematical analysis for two-level system particles that serve as building blocks for multi-particle qubits is no longer valid.

## 4 The quest for anyon statistics

In this chapter we present the attempts made to implement a universal set of quantum gates on multi-spin qubits using spin braiding. We use, as a target set of quantum gates, the universal set that is constructed in Ref. [9]:

$$G = \left\{ \underbrace{\{\hat{\sigma}_x, \hat{\sigma}_y, \hat{\sigma}_z, e^{i\frac{\pi}{4}\hat{\sigma}_z}\}}_{\text{single qubit gates}}, \underbrace{e^{i\frac{\pi}{4}\hat{\sigma}_x \times \hat{\sigma}_x}}_{\text{two-qubit gate}} \right\}. \quad (4.1)$$

We first check whether we can reproduce the “Ising-type” anyon exchange statistics with spin braiding in Section 4.1. We find that it cannot be done in Section 4.1.2.

From there on, we try to implement the set of operations directly using different computational mapping. For this, we look for spin-braiding operators  $B$  that have similar characteristics as the target operators  $G$  (see Section 4.2). We, then, turn to list the non-linear properties of a computational mapping that permit such a universal set of operations to exist (see Section 4.3).

### 4.1 Anyon statistics are not reproducible (a “false quest”)

If we could produce the non-Abelian  $\nu = 5/2$  anyon exchange statistics of “Ising-type” anyons with spin braiding, this would be a significant step toward using the results of Ref. [9] to produce the target operator set  $G$ .<sup>5</sup>

The “Ising-type” anyons are two-dimensional quasi-particles that obey the following exchange (braiding) statistics:

Let  $\hat{B}_{i,j}$  be the operator exchanging particles  $i$  and  $j$ . It was shown in Ref. [19] that  $\hat{B}_{i,j} = e^{i\frac{\pi}{4}\hat{\sigma}_z^{\{i,j\}}}$  where  $\hat{\sigma}_z^{\{i,j\}}$  is the spinor representation of some combination of Moore-Read wave functions for the quasi-particles  $i$  and  $j$ . Furthermore,  $\hat{\sigma}_z^{\{i,j\}}$  has a representation in terms of Majorana fermions  $\hat{\sigma}_z^{\{i,j\}} = \hat{c}_i \hat{c}_j$  and so:

$$\hat{B}_{i,j} = e^{i\frac{\pi}{4}\hat{\sigma}_z^{\{i,j\}}} = e^{-\frac{\pi}{4}\hat{c}_i \hat{c}_j} = \frac{1}{\sqrt{2}}(1 - \hat{c}_i \hat{c}_j), \quad (4.2)$$

---

<sup>5</sup>“Ising-type” anyon braiding statistics is not sufficient for producing universal quantum computation. In Ref. [9] parity measurements are required as well.

where  $\hat{c}_i, \hat{c}_j$  are Majorana fermions that obey:

$$\hat{c}_i^\dagger = \hat{c}_i, \quad \hat{c}_i^2 = \mathbf{1}, \quad \{\hat{c}_i, \hat{c}_j\} = 2\delta_{ij}. \quad (4.3)$$

Thus, in order to mimic the  $\nu = 5/2$  non-Abelian anyon braiding statistics, our spin-braiding must fulfill the following conditions:

- The spin braiding must induce non-Abelian exchange.
- The spin braiding must have an eight-fold application length, i.e. the operator must be cyclic and after eight applications return to the identity:

$$\hat{B}_{i,j}^4 = -\mathbf{1}, \quad (4.4)$$

$$\hat{B}_{i,j}^8 = \mathbf{1}. \quad (4.5)$$

- The spin braiding must have a braid group representation, i.e. it must, non-trivially, fulfill the Yang-Baxter relations:

$$\hat{B}_i \hat{B}_j = \hat{B}_j \hat{B}_i \text{ for } |i - j| > 2, \quad (4.6)$$

$$\hat{B}_i \hat{B}_{i+1} \hat{B}_i = \hat{B}_{i+1} \hat{B}_i \hat{B}_{i+1}, \quad (4.7)$$

where  $\hat{B}_i$  is the non-trivial braiding of particles  $i$  and  $i + 1$ , i.e.  $\hat{B}_i \hat{B}_{i+1} \neq \hat{B}_{i+1} \hat{B}_i$ .

- The spin braiding must have a similar Majorana decomposition.

We prove here that such a Majorana decomposition does not exist for any spin-braiding operation. We prove it for the case of a two-spin qubit,  $N = 2$ , and generalize for any qubit size.

#### 4.1.1 A non-Abelian spin-braiding scheme

To emphasize the impossibility of reproducing the ‘‘Ising-type’’ anyon braiding statistics by using spin braiding. We present a spin-braiding operator over a two-spin qubit that fulfills the first three of the above conditions but fails to have a similar Majorana decomposition.

Fig. 3 shows the clockwise spin braiding, where, the spin going from left to right is rotated by  $\pi/4$  along  $\sigma_z$  and the spin moving from right to left simply swaps places. The counter-clockwise exchange is a simple spin swap.

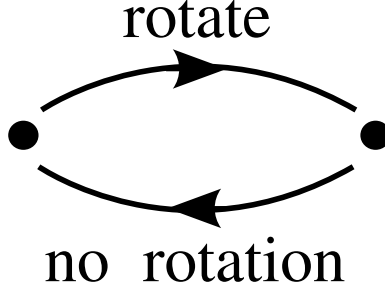


Figure 3: A non-Abelian spin-braiding scheme - In the figure the clockwise exchange is seen where the spin going from left to right is rotated by  $\pi/4$  around  $\hat{z}$  and the one moving from right to left is untouched.

We obtain the following operator for the clockwise exchange:

$$\hat{B}_i = \hat{B}_i(e^{i\frac{\pi}{4}\hat{\sigma}_z^i} \times \mathbf{1}), \quad (4.8)$$

where  $\hat{B}_i$  is the simple spin exchange and  $\hat{\sigma}_z^i$  is the spin operator which acts on the spin at location  $i$ .

The braiding is indeed non-Abelian by definition and  $\hat{B}^8 = 1$ . It also fulfills the Yang-Baxter relations non-trivially (as shown in Fig. 4).

#### 4.1.2 Braiding spins cannot mimic Ising-anyon braiding statistics

We choose our qubit to be composed of two spins ( $N = 2$ ) and check whether for  $\hat{B} = \hat{B}_1$  we can find an Ising-type anyon Majorana representation, i.e. whether there is a representation of the form

$$\hat{B} = e^{-\frac{\pi}{4}\hat{c}_i\hat{c}_{i+1}} = \frac{1}{\sqrt{2}}(\mathbf{1} - \hat{c}_i\hat{c}_{i+1}). \quad (4.9)$$

To check this, we note that  $\hat{B}$  can be written as

$$\hat{B} = \frac{1}{\sqrt{2}}(\mathbf{1} - \hat{A}). \quad (4.10)$$

Using the Majorana fermion relations from Eq. (4.3) we find that

$$\hat{A} + \hat{A}^\dagger = 0, \quad (4.11)$$

$$\begin{array}{ccc}
 0 & 0 & 0 \\
 \times & & | \\
 0 & \frac{\pi}{4} & 0 \\
 | & & \times \\
 0 & 0 & \frac{\pi}{2} \\
 \times & & | \\
 0 & \frac{\pi}{4} & \frac{\pi}{2}
 \end{array}
 =
 \begin{array}{ccc}
 0 & 0 & 0 \\
 | & & \times \\
 0 & 0 & \frac{\pi}{4} \\
 \times & & | \\
 0 & \frac{\pi}{4} & \frac{\pi}{4} \\
 | & & \times \\
 0 & \frac{\pi}{4} & \frac{\pi}{2}
 \end{array}$$

Figure 4: Proof that the spin-braiding operation fulfills the Yang-Baxter relations - Once a new braiding scheme is devised, one must make sure that the Yang-Baxter relations remain valid. Here, we see that our spin-braiding scheme indeed satisfies Eq. (4.7) non-trivially (i.e. equality holds only after the full set of braiding operation). The proof is read from top to bottom. Each of the three columns represents a location that the spin can be in. The number represents the phase of the state of the spin that occupies that location. Between rows, the spin braiding is operated on two of the spins (represented by an X) while the third spin stays in place (represented by a line).

is a necessary condition (but not sufficient) for such a Majorana representation. Below, however, we show that this condition is violated and a representation in terms of Majorana fermions is not possible. Thus, we prove that spin-braiding operations cannot mimic Ising-anyon braiding.

We proceed as follows: We write  $\hat{B}$  in its matrix form over the normal multi-spin basis  $\{|\uparrow\uparrow\rangle, |\uparrow\downarrow\rangle, |\downarrow\uparrow\rangle, |\downarrow\downarrow\rangle\}$ :

$$\begin{aligned} \hat{B} &= \begin{pmatrix} 1 & 0 & 0 & 0 \\ 0 & 0 & 1 & 0 \\ 0 & 1 & 0 & 0 \\ 0 & 0 & 0 & 1 \end{pmatrix} \begin{pmatrix} e^{i\frac{\pi}{4}} & & & \\ & e^{i\frac{\pi}{4}} & & \\ & & e^{-i\frac{\pi}{4}} & \\ & & & e^{-i\frac{\pi}{4}} \end{pmatrix} \\ &= \begin{pmatrix} e^{i\frac{\pi}{4}} & 0 & 0 & 0 \\ 0 & 0 & e^{-i\frac{\pi}{4}} & 0 \\ 0 & e^{i\frac{\pi}{4}} & 0 & 0 \\ 0 & 0 & 0 & e^{-i\frac{\pi}{4}} \end{pmatrix} = \frac{1}{\sqrt{2}} \begin{pmatrix} 1+i & 0 & 0 & 0 \\ 0 & 0 & 1-i & 0 \\ 0 & 1+i & 0 & 0 \\ 0 & 0 & 0 & 1-i \end{pmatrix}. \end{aligned} \quad (4.12)$$

Thus

$$\hat{A} = \begin{pmatrix} -i & 0 & 0 & 0 \\ 0 & 1 & -1+i & 0 \\ 0 & -1-i & 1 & 0 \\ 0 & 0 & 0 & i \end{pmatrix}, \quad (4.13)$$

and the necessary condition from Eq. (4.11) is violated:

$$\hat{A} + \hat{A}^\dagger = \begin{pmatrix} 0 & 0 & 0 & 0 \\ 0 & 2 & -2+2i & 0 \\ 0 & -2-2i & 2 & 0 \\ 0 & 0 & 0 & 0 \end{pmatrix}. \quad (4.14)$$

We note that, once the condition  $\hat{A} + \hat{A}^\dagger = 0$  is violated over the normal spin basis, it is violated for the whole Hilbert space as the condition is insensitive to local unitary basis transformations.

The violation comes from the fact that the spin-braiding operator  $\hat{B}$  has zero elements on the diagonal and so the matrix  $\hat{A}$  has ones there (see Eq. (4.10)).

Spin-braiding matrices will always have diagonal zero elements in the normal spin basis representation because of the fact that spin permutation operators map normal spin basis states either to themselves or to other normal spin

---

basis states. The latter produces a zero element on the diagonal. Thus, we can generalize the contradiction of the constraint from Eq. (4.11) to any  $N$ -spin qubit braiding scheme. Therefore, spin braiding cannot mimic Ising-type anyon braiding.

However, the contradiction of the Majorana decomposition constraint occurs at the operator level that operates on the whole Hilbert space. Yet, if we choose a projective computational mapping on a subspace which is diagonal in the normal spin basis, we do not break the constraint. However, we risk leaving this subspace on subsequent braiding with additional qubits.

Such is the case for the operator  $\hat{B}$ , when we use a projective computational mapping (see Section 3.1.1) to encode a qubit on the stationary normal basis states of  $\{|\uparrow\uparrow\rangle \rightarrow |1\rangle, |\downarrow\downarrow\rangle \rightarrow |0\rangle\}$ . These states are indeed eigenstates of  $\hat{B}$  over which the constraint  $\hat{A} + \hat{A}^\dagger = 0$  is satisfied. Moreover, their eigenvalues are  $e^{\pm i\frac{\pi}{4}}$ , which result in operator equivalence between  $\hat{B}$  and computational rotation gate  $\hat{g} = e^{i\frac{\pi}{4}\hat{\sigma}^z}$ . Thus, fulfilling part of the requirements defined in Eq. (3.8).

In this subspace though, we cannot carry out braiding between two qubits without leaving the computational space. This is shown in the case where we have two qubits in orthogonal states, e.g.  $|\uparrow\uparrow\rangle_1 |\downarrow\downarrow\rangle_2$ . Thus, after braiding spins 2 and 3 we end in a state  $e^{i\frac{\pi}{4}} |\uparrow\downarrow\rangle_1 |\uparrow\downarrow\rangle_2$  that cannot be decomposed by the basis states of the computational space  $\{|\uparrow\uparrow\rangle, |\downarrow\downarrow\rangle\}$ .

### 4.1.3 Summary

We have devised a non-Abelian braiding of spins and have shown that it cannot be interpreted as exchange of ‘‘Ising-type’’ anyons. This result can be generalized for any braiding of spins, proving that we cannot mimic the ‘‘Ising-type’’ anyon exchange statistics with the braiding of spins.

We have also shown an example of a projected subspace over which the spin-braiding satisfies the ‘‘Ising-type’’ anyon exchange statistics. However, the braiding scheme could not be extended to braid spins between different qubits without breaking out of the computational subspace, thus, emphasizing the difference between ‘‘Ising-type’’ anyons, which are identical particles until fused together, to spins that differ by their spin orientation.

As the Yang-Baxter relations are non-trivially fulfilled by the spin-braiding, we achieve some braiding statistics, but not of Ising type anyons. It might be

possible to use these statistics to construct a different computation scheme than that of Ref. [9]. Yet, we will see in Section 4.3 that this is highly unlikely.

## 4.2 Spin permutations as qubit rotations and two-qubit entanglement

We have seen that we cannot reproduce the anyon braiding statistics using spin braiding. We can still use our multi-qubit scheme to target the universal set of gates  $G$  in Eq. (4.1) directly. We set out to satisfy Eq. (3.8) with a given set of physical spin-braiding operators  $B$ . We therefore rewrite Eq. (3.8) for our  $N$ -qubit system with the given physical and computational gates:

$$G = \{\hat{\sigma}_x, \hat{\sigma}_y, \hat{\sigma}_z, e^{i\frac{\pi}{4}\hat{\sigma}_z}, e^{i\frac{\pi}{4}\hat{\sigma}_x \times \hat{\sigma}_x}\} \quad (4.15)$$

$$B = \{\text{spin-braiding operations}\} \quad (4.16)$$

$$\forall \hat{g} \in G \exists \hat{b} \in B \quad \hat{g}f(|\psi\rangle_N) \equiv f(\hat{b}|\psi\rangle_N) \quad (4.17)$$

Hence, we are looking for elaborate spin-braiding procedures  $B$  that have similar characteristics as the target operators  $G$  under some computational mapping  $f$ .

As the size of the qubit grows, we have a wider variety in choice of spin-braiding  $B$  and computational mappings  $f$ . We saw in Section 4.1 a spin-braiding operator on a two-spin qubit that implemented a single-qubit rotation, but failed in implementing more gates under that computational mapping. We therefore limit ourselves to a subset of  $B$  composed of all spin permutations and leave the computational mapping undefined. From this, we hope to learn about requirements on the size of the system.

### 4.2.1 Single qubit rotation

We wish to find a spin permutation operator  $\hat{B}$  that satisfies Eq. (4.17) for the single qubit rotation operator  $\hat{g} = e^{i\frac{\pi}{4}\hat{\sigma}_z}$ . We would like its eigenvalues to be equal to our target operator's eigenvalues and seek to keep our computational interpretations  $f : \mathcal{H}_n \rightarrow \mathcal{H}_2^{comp}$ . (where  $n = 2^N$  and  $N$  is the number of spins that compose the qubit) as simple as possible.

The target operator  $\hat{g}$  has eigenvalues  $e^{\pm i\frac{\pi}{4}}$  and is a cyclic operator of length-8 ( $\hat{g}^4 = -\mathbf{1}$ ). The shortest braiding operator (permutation) that has a length-8 is a cycle of eight  $\hat{B} = (1\ 2\ 3\ 4\ 5\ 6\ 7\ 8)$ . Thus, our pseudo-particle should contain at least 8 spins ( $N \geq 8 \Rightarrow n \geq 256$ ).

We write down our operator in matrix form in the  $N$ -spins normal basis space ( $\hat{B} = \mathbb{M}_{256 \times 256}$ ) and diagonalize it. Diagonalizing a length-8 permutation operator results in eight sub-blocks corresponding to eight eigenvalues. Two of these sub-blocks have eigenvalues  $e^{\pm i\frac{\pi}{4}}$ .

We can now define our computational interpretation  $f : \mathcal{H}_{256} \rightarrow \mathcal{H}_2^{comp}$  over the eigenstates corresponding to these sub-blocks:

$$f(|\psi\rangle_8) := \begin{cases} 0 & \text{if } |\psi\rangle_8 \in \ker(f) = \{|\psi\rangle_8 : \hat{B}|\psi\rangle_8 \neq e^{\pm i\frac{\pi}{4}}|\psi\rangle_8\}, \\ |0\rangle & \text{if } \hat{B}|\psi\rangle_8 = e^{-i\frac{\pi}{4}}|\psi\rangle_8, \\ |1\rangle & \text{if } \hat{B}|\psi\rangle_8 = e^{i\frac{\pi}{4}}|\psi\rangle_8. \end{cases} \quad (4.18)$$

Where the eigenstates are well-defined entangled states of our 8-spin pseudo-particle:

$$|\psi\rangle_8 = \sum_{\sigma_1, \dots, \sigma_8 = \uparrow, \downarrow} \beta_{\sigma_1, \dots, \sigma_8} |\sigma_1, \dots, \sigma_8\rangle. \quad (4.19)$$

We obtain the operator equivalence:

$$\hat{g}f(|\psi\rangle_8) \equiv f(\hat{B}|\psi\rangle_8). \quad (4.20)$$

The sub-blocks related to each eigenvalue are multi-dimensional. Hence, each representative from this block is a valid computational state.

We have presented here the case where  $N = 8$ , but we could also take a larger qubit  $N > 8$  on which we operate with a length-8 permutation. The operator will still have eight sub-blocks, corresponding to eight eigenvalues, but of larger dimensions.

#### 4.2.2 two-qubit entanglement

Now that we have partially defined the computational mapping  $f$  on the eight-spin qubit system, we wish to find whether we can create the two-qubit entangling operation  $\hat{g}_{\hat{\sigma}_x, \hat{\sigma}_x} = e^{i\frac{\pi}{4}\hat{\sigma}_{1,x} \times \hat{\sigma}_{2,x}}$ . For this, we need to double the computational space to contain two qubits and define an identical single

qubit rotation scheme on the second qubit (additional eight spins):

$$\hat{B}_2 = \quad (9 \ 10 \ 11 \ 12 \ 13 \ 14 \ 15 \ 16), \quad (4.21)$$

$$\hat{g}_2 = \quad e^{i\frac{\pi}{4}\mathbf{1}\times\hat{\sigma}_{2,z}}, \quad (4.22)$$

$$f_2(|\psi\rangle_{16}) := \begin{cases} 0 & \text{if } |\psi\rangle_{16} \in \ker(f_2) = \{|\psi\rangle_{16} : \hat{B}_2|\psi\rangle_{16} \neq e^{\pm i\frac{\pi}{4}}|\psi\rangle_{16}\}, \\ |\tilde{\alpha}, 0\rangle & \text{if } \hat{B}_2|\psi\rangle_{16} = e^{-i\frac{\pi}{4}}|\psi\rangle_{16}, \\ |\tilde{\alpha}, 1\rangle & \text{if } \hat{B}_2|\psi\rangle_{16} = e^{i\frac{\pi}{4}}|\psi\rangle_{16}. \end{cases} \quad (4.23)$$

$\tilde{\alpha} \in \{0, 1\},$

adding a subscript 1 to the first qubit operators, we can define the two-qubit mapping  $\tilde{f} = f_1 \times f_2 : \mathcal{H}_{65536} \rightarrow \mathcal{H}_4^{comp}$  that fulfills:

$$\hat{g}_1(\tilde{f}|\psi\rangle_{16}) \equiv \tilde{f}(\hat{B}_1|\psi\rangle_{16}), \quad (4.24)$$

$$\hat{g}_2(\tilde{f}|\psi\rangle_{16}) \equiv \tilde{f}(\hat{B}_2|\psi\rangle_{16}). \quad (4.25)$$

Up to now, we projected our physical space (of dimension 65,536) onto a subspace spanned by eigenstates of  $\hat{B}_1$  and  $\hat{B}_2$  with eigenvalues  $e^{\pm i\frac{\pi}{4}}$ . This computational subspace is divided into four spaces corresponding to the four combinations of these eigenvalues. Each block of the four has a dimension 900 (spanned by 900 eigenstates) and has been associated with a two-qubit state (depending on the eigenvalues). Hence, our computational mapping  $\tilde{f}$  is well defined up to a degeneracy in the computational subspaces. We are therefore looking for a braiding operation  $\hat{\hat{B}}$  that will be computationally equivalent to  $\hat{g}_{\hat{\sigma}_x, \hat{\sigma}_x}$  for some states in our computational subspace.

We note that  $\hat{g}_{\hat{\sigma}_x, \hat{\sigma}_x}$  is also an operator of cycle-eight. Thus, we are looking for another eight-cycle permutation of spins. As our qubits are identical and we seek to reach entanglement with the exchange of spins between them, we favour a symmetric permutation of 4 spins from each qubit (we have also tried non-symmetric permutations). The spin building blocks are identical particles, so without loss of generality, the symmetric permutation operator which is a candidate for the two-qubit operation is  $\hat{\hat{B}} = (5 \ 6 \ 7 \ 8 \ 9 \ 10 \ 11 \ 12)$ .

Our goal is to find a subspace of the computational space that is closed under  $\hat{\hat{B}}, \hat{B}_1$  and  $\hat{B}_2$ . If such a subspace is found, we need to make sure that we have an operator equality for all three operators over some part of this closed subspace. For this we can check whether  $\hat{\hat{B}}$  is closed under the computational space (spanned by eigenstates of  $\hat{B}_1$  and  $\hat{B}_2$  with eigenvalues  $e^{\pm i\frac{\pi}{4}}$ ). Thereafter, we are left only with the need to check whether operator

equality between  $\hat{B}$  and  $\hat{g}_{\hat{\sigma}_x, \hat{\sigma}_x}$  exists for some representatives from the closed subspace as we have all the demands for  $\hat{B}_1$  and  $\hat{B}_2$  settled by the choice of the computational space.

Finding such a closed space is rather unlikely and is quite difficult (due to the high dimensionality). However, we have written a numerical code for this process in order to provide a systematic proof of this claim. The algorithm is as follows:

1. Diagonalize  $\hat{B}_1$  and find its eigenstates.
2. Create a two-qubit/16-spin tensor space from the eigenstates and arrange them in computational sub-blocks.
3. Transform  $\hat{B}$  to the new eigenstate basis and see whether it is closed for some states from our computational sub-block.

We applied this algorithm on qubits composed of  $2 \leq N \leq 8$ , where, for the  $2 \leq N < 8$  qubits, we targeted similar qubit rotations with a shorter cycle (i.e.  $e^{i\frac{2\pi}{N}\sigma_z}$ ). We did not, however, find invariant states under the application of the two-qubit permutation. The permutation operator leaves just a small part of the each candidate state within the computational space ( $\approx 20\%$ ), such that even error correction schemes are out of the question.

### 4.2.3 Summary

We have found that in a naive setup, where we find a spin-braiding operator that has eigenvalues similar to a target single-qubit operator, we are soon forced to choose a computational representation that is not flexible enough to allow us to perform two-qubit entanglement on this system without leaving the computational space.

For further examination of the problem, one has to increase the number of spins composing the qubit, while keeping the operation to a cycle of eight. Thus, more degrees of freedom in the choice of  $\tilde{f}$  will be achieved. This means, however, that the system size and computation time will increase exponentially.

We must also note that, even if such a subspace of states can be found, a practical realization of a specifically defined  $N$ -spin entangled state ( $N \geq 8$ )

would be hard to achieve. Once achieved, though, our target operations could be achieved within this subspace only with the permutation of spins.

### 4.3 The properties of a non-linear computational mapping

Until now, we have seen in this chapter examples of spin-braiding operators which forced us to choose a specific too strict computational mapping  $f$  when we implemented the operator  $\hat{g} = e^{i\frac{\pi}{4}\hat{\sigma}_z}$ . Under this qubit encoding, it became impossible to implement universal quantum computation without leaving the computational space with our proposed operations.

We now take a different approach in which we search for the minimal constraints on a general computational mapping  $f$ . Our only initial condition is that we choose  $f$  such that we divide the complete multi-spin Hilbert space into two (computational) blocks, without projecting on a smaller computational subspace. Under this condition, we seek to learn about the non-linear properties that  $f$  must fulfill.

In other words, we seek an orthogonal decomposition of our multi-spin Hilbert space into  $\mathcal{H}_0$  and  $\mathcal{H}_1$ , such that:

$$\mathcal{H}_0 \perp \mathcal{H}_1 \text{ and } \mathcal{H}_0 \oplus \mathcal{H}_1 = \mathcal{H}. \quad (4.26)$$

A scheme like this is favorable, as we do not have to worry about leaving the computational space by operations on the qubit (as we have seen in Sections 4.1,4.2) and we do not need to create specially entangled states that belong to our computational projected state (as we saw in Section 4.2).

A decomposition into the computational spaces is part of the definition of  $f$  and we can list the conditions that  $f$  must fulfill as follows:

1.  **$f$  must keep the norm of the states:**

$$\|f(|\psi\rangle_N)\| = \|\psi\rangle_2\| \Rightarrow \|f(\lambda|\psi\rangle_N)\| = |\lambda| \|f(|\psi\rangle_2)\|. \quad (4.27)$$

2. **The computational mapping cannot be linear:**

We would like to define  $f$  as a linear mapping that operates on a basis of states  $\{|\psi\rangle_i\}_{i=1}^n$  (and thus on the entire space):

$$\forall i f(|\psi_i\rangle) := \begin{cases} |0\rangle & \text{if } |\psi_i\rangle \in \mathcal{H}_0 = \text{span}\{\{|\psi\rangle_i\}_{i=1}^n\}, \\ |1\rangle & \text{if } |\psi_i\rangle \in \mathcal{H}_1 = \text{span}\{\{|\psi\rangle_i\}_{i=r+1}^n\}. \end{cases} \quad (4.28)$$

Let  $|\psi\rangle_N$  be an arbitrary state. We can decompose it in the basis:

$$|\psi\rangle_N = \sum_{j=1}^n \beta_j |\psi_j\rangle, \quad (4.29)$$

where

$$\sum_{j=1}^n |\beta_j|^2 = 1. \quad (4.30)$$

Under the linear definition of  $f$ :

$$f(|\psi\rangle_N) = f(\sum_{j=1}^r \beta_j |\psi_j\rangle + \sum_{j=r+1}^n \beta_j |\psi_j\rangle) \quad (4.31)$$

$$= \sum_{j=1}^r \beta_j f(|\psi_j\rangle) + \sum_{j=r+1}^n \beta_j f(|\psi_j\rangle) \quad (4.32)$$

$$= \sum_{j=1}^r \beta_j |0\rangle + \sum_{j=r+1}^n \beta_j |1\rangle \quad (4.33)$$

$$= \gamma |0\rangle + \delta |1\rangle. \quad (4.34)$$

where

$$\gamma = \sum_{j=1}^r \beta_j \quad \delta = \sum_{j=r+1}^n \beta_j. \quad (4.35)$$

From the triangle inequality:

$$|\gamma|^2 + |\delta|^2 \leq \sum_{j=1}^n |\beta_j|^2 = 1. \quad (4.36)$$

Therefore, a linear  $f$  does not preserve the norm of non-basis states and we cannot use it as our computational mapping.

**3. A non-linear  $f$  with linearity over the computational blocks:**

We want to perform quantum mechanical computation which is linear. Therefore, the mapping  $f$ , despite being non-linear, must be linear with respect to the decomposition into  $\mathcal{H}_0$  and  $\mathcal{H}_1$ .

Let  $|\psi\rangle_N$  be a normalized  $N$ -spin state. It can be decomposed into  $\mathcal{H}_0$  and  $\mathcal{H}_1$ :

$$|\psi\rangle_N = \alpha |\psi\rangle_N^0 + \beta |\psi\rangle_N^1 \quad (4.37)$$

where  $|\psi\rangle_N^0 \in \mathcal{H}_0$ ,  $|\psi\rangle_N^1 \in \mathcal{H}_1$  and  $|\alpha|^2 + |\beta|^2 = 1$ .

Therefore,

$$f(|\psi\rangle_N) = f(\alpha|\psi\rangle_N^0) + f(\beta|\psi\rangle_N^1). \quad (4.38)$$

As  $f$  keeps the norm we obtain:

$$f(|\psi\rangle_N) = |\alpha||0\rangle + |\beta||1\rangle \quad \text{where } |\alpha|^2 + |\beta|^2 = 1, \quad (4.39)$$

and  $f$  is linear over the computational block decomposition.

#### 4. Definition of phase:

In order to perform quantum computation, we must define the phase of the computational states. There are many ways to do this as the cardinality of the group of non-linear mappings  $f : \mathcal{H}_n \rightarrow \mathcal{H}_2$  is infinite. However, we must keep in mind the previous condition that our mapping should remain linear over the computational blocks, and therefore, we choose to define the phase in an analogous way to the quantum mechanical wave function phase:

Let  $\Psi(x)$  be a wave function. Its phase depends on the choice of the basis  $|x\rangle$ :

$$\Psi(x) = \langle x|\psi\rangle = |\langle x|\psi\rangle| e^{i\phi(x)}, \quad (4.40)$$

where,

$$\phi(x) = \arg(\langle x|\psi\rangle). \quad (4.41)$$

We can carry this method over to our mapping  $f$  by imposing the following:

$$f(|\psi\rangle_N) = f(\alpha|\psi\rangle_N^0) + f(\beta|\psi\rangle_N^1) \quad (4.42)$$

$$= |\alpha|e^{i\phi_0(x_0)}|0\rangle + |\beta|e^{i\phi_1(x_1)}|1\rangle, \quad (4.43)$$

where  $|x_0\rangle, |x_1\rangle$  are basis states chosen out of  $\mathcal{H}_0, \mathcal{H}_1$  respectively such that:

$$\phi_0(x_0) = \arg(\langle x_0|\psi\rangle_N^0), \quad (4.44)$$

$$\phi_1(x_1) = \arg(\langle x_1|\psi\rangle_N^1). \quad (4.45)$$

We have defined the phase in such a way since the phase of the mapping must be defined on a physical state (on  $|\psi\rangle_N$ ) and not on a computational state (on  $|\psi\rangle_2$ ). Thus, we select two reference states in  $\mathcal{H}_0$  and

$\mathcal{H}_1$  and use them to define a phase for the computational blocks, as is done in quantum mechanics.

We thus impose that all  $|\psi\rangle_N^0$  which have no  $|x_0\rangle$  component, i.e.  $\langle x_0|\psi\rangle_N^0 = 0$ , have phase zero. The same applies for the  $\mathcal{H}_1$  block with  $|\psi\rangle_N^1$  which have no  $|x_1\rangle$  component.

We also note that the reference states are also phase-less, i.e.  $\arg(\langle x_0|x_0\rangle) = 0$  and  $\arg(\langle x_1|x_1\rangle) = 0$ .

### 4.3.1 Operations

In the previous section, we found that the mapping  $f$  must fulfill many conditions in the way we defined it. We do have, however, a freedom in the choice of the division into  $\mathcal{H}_0, \mathcal{H}_1$  and in the choice of representatives defining the computational phases  $\phi_0(x_0), \phi_1(x_1)$ . We can, therefore, proceed to attempt to implement the target operations.

Our first target operator  $\hat{g}$  only adds a phase to its eigenstates (i.e.  $\hat{g}|0\rangle = e^{i\frac{\pi}{4}}|0\rangle$  and  $\hat{g}|1\rangle = e^{-i\frac{\pi}{4}}|1\rangle$ ), thus we need a physical operation  $\hat{b} \in B$  such that:

$$\hat{b}|\psi\rangle_N \in \begin{cases} \mathcal{H}_0 & \text{if } |\psi\rangle_N \in \mathcal{H}_0, \\ \mathcal{H}_1 & \text{if } |\psi\rangle_N \in \mathcal{H}_1. \end{cases} \quad (4.46)$$

Our goal is to have an operator equality over the two spaces

$$\forall |\psi\rangle_N \quad f(\hat{b}|\psi\rangle_N) \equiv \hat{g}f(|\psi\rangle_N). \quad (4.47)$$

We search for the requirements on the definition of  $f$ :

Let  $|\psi\rangle_N^0$  be a phase-less state in  $\mathcal{H}_0$  under the mapping of  $f$  (i.e.  $\phi_0(x_0) = 0 \iff \langle x_0|\psi\rangle_N^0 \in \mathbb{R}$ ).

From Eq. (4.47), we require that

$$f(\hat{b}|\psi\rangle_N^0) \equiv \hat{g}f(|\psi\rangle_N^0) = e^{i\frac{\pi}{4}}|0\rangle. \quad (4.48)$$

Additionally,  $\hat{b}$  is a well-defined physical operation that changes the physical states. Thus:

$$f(\hat{b}|\psi\rangle_N^0) = f(|\tilde{\psi}\rangle_N), \quad (4.49)$$

where  $\hat{b}|\psi\rangle_N^0 = |\tilde{\psi}\rangle_N$  is a general state in  $\mathcal{H}$ , i.e. it does not belong to a specific computational block and might have a phase.

We can decompose  $|\tilde{\psi}\rangle_N$  into computational blocks and from the linearity of  $f$  over these blocks we can rewrite Eq. (4.49):

$$f(|\tilde{\psi}\rangle_N) = f(\alpha |\tilde{\psi}\rangle_N^0) + f(\beta |\tilde{\psi}\rangle_N^1). \quad (4.50)$$

In order to impose the operator equality from Eq. (4.47), we compare Eq. (4.48) with Eq. (4.50) and find that the following two constraints are imposed:

1.  **$\hat{b}$  must be in a two-block diagonal form**

Under the definition of  $f$ , for the operator equality to exist,  $\hat{b}$  must not mix the computational blocks, i.e.  $\beta$  is set to zero in Eq. (4.50). This means that  $\hat{b}$  must be in a two-block diagonal form over the basis that defines the division into  $\mathcal{H}_0$  and  $\mathcal{H}_1$ .

2.  **$|x_0\rangle, |x_1\rangle$  must be constants of  $\hat{b}$ , by which we mean the following**

We can decompose the remaining state in Eq. (4.50) into two parts within its computational block:

$$f(\alpha |\tilde{\psi}\rangle_N^0) = f(\rho |x_0\rangle + \rho_\perp |x_{0,\perp}\rangle) = e^{i \arg(\rho)} |0\rangle, \quad (4.51)$$

and obtain that:

$$|\alpha| = \sqrt{|\rho|^2 + |\rho_\perp|^2} = 1, \quad (4.52)$$

$$\arg(\rho) = \frac{\pi}{4}. \quad (4.53)$$

The condition in Eq. (4.52) is not surprising. It repeats the previous constraint of the two-block diagonal form of the operator  $\hat{b}$ . In order to derive the implication of the condition in Eq. (4.53) on  $f$  and  $\hat{b}$ , we present the following two cases:

- From the case in which  $|\psi\rangle_N^0 = |x_0\rangle$ :

$$f(\hat{b} |x_0\rangle) = f(\rho |x_0\rangle + \rho_\perp |x_{0,\perp}\rangle), \quad (4.54)$$

we learn that  $|x_0\rangle$  must remain a part of the decomposition of  $\hat{b}(|x_0\rangle)$ , i.e.  $|\rho| \neq 0$ . It must also accumulate a  $e^{i\frac{\pi}{4}}$  phase, i.e.  $\arg(\rho) = e^{i\frac{\pi}{4}}$ .

- From the case where  $\langle x_0|\psi\rangle_N^0 = 0$ :

$$f(\hat{b} |\psi\rangle_N^0) = f(\rho |x_0\rangle + \rho_\perp |x_{0,\perp}\rangle), \quad (4.55)$$

we learn that  $\hat{b}$  applied on any state in  $\mathcal{H}_0$  must produce a part containing  $|x_0\rangle$  with a  $e^{i\frac{\pi}{4}}$  phase factor.

### 4.3.2 Computational division by operator eigenstates

We have seen in the previous attempts in this chapter that we tried intuitively to divide the Hilbert space into  $\mathcal{H}_0$  and  $\mathcal{H}_1$  that are spanned by eigenvectors  $\{|\psi_i\rangle\}_{i=1}^n$  of  $\hat{b}$  where:

$$\mathcal{H}_0 = \text{span}\{|\psi_i\rangle\}_{i=1}^r, \quad (4.56)$$

$$\mathcal{H}_1 = \text{span}\{|\psi_i\rangle\}_{i=r+1}^n, \quad (4.57)$$

$$\hat{b}|\psi_i\rangle = e^{\pm i\frac{\pi}{4}}|\psi_i\rangle. \quad (4.58)$$

This is a special case of the above setup with:

$$|x_0\rangle = \frac{1}{\sqrt{r}} \sum_{j=1}^r |\psi_j\rangle \quad (4.59)$$

$$|x_1\rangle = \frac{1}{\sqrt{n-r-1}} \sum_{j=r+1}^n |\psi_j\rangle. \quad (4.60)$$

However, as we have seen, it constrains the system and blocks us from adding operations to the set of implemented quantum gates.

### 4.3.3 Conclusions

We discussed the minimal constraints on our computational mapping when we do not project the multi-dimensional system to a two-level system. This discussion is a general overview of the non-linear constraints of such mappings. Therefore, the discussion is relevant for any type of physical operator  $\hat{b}$  and may serve as a basic guideline for any attempt to find non-linear mappings between Hilbert spaces that impose operator equivalence.

There are many ways to choose such a non-linear function. However, we chose the intuitive mapping sub-group that is inspired by the postulates of quantum mechanics. Under this approach we showed the list of constraints that the mappings must fulfill, i.e., the mappings must preserve the norms of the states, keep linearity over sub-blocks, and define a computational phase. From this, we found that the mapping itself is already highly constrained and limits the possible candidates for operators that can serve as quantum gates. The physical operators (spin braiding in our case) must have the needed eigenvalues of the computational operation embedded in their definition. Therefore, we have to divide the physical Hilbert space into

computational sub-blocks in relation to a specific physical operator. This further constrains our computational mapping's definition in a way that hinders the implementation of additional quantum gates.

The impossibility to implement more than one quantum gate has been shown in all the attempts in this chapter. The computational mappings divided the Hilbert space into computational blocks in relation to eigenstates of an operator and could not introduce additional quantum gates. However, these mappings exceed from the minimal set of constraints introduced in this section and demand that the operators be diagonal with the needed eigenvalues. One could, therefore, work with the less intuitive minimal set of constraints given in Section 4.3.1 and check whether additional operators can be implemented.

At this point, though, we choose to leave this route. It demands a systematic iteration of all the possible mappings that fulfill this set of constraints. For each such mapping one should test all the possible physical operations that might have the needed eigenvalues embedded in their definition, i.e., they must fulfill the set of constraints under a specific basis choice. Such a process is not based on any physical insight and is no longer researched in this thesis.

#### 4.4 Summary

We have shown that spin-braiding cannot replicate "Ising-type" anyon exchange statistics. This led us to try to directly implement a universal set of gates over different multi-spin qubits using different spin-braiding operations. In each of our attempts we were forced to leave the assigned computational space and so we failed to implement the universal set of gates. Thus, we went on to a general study of the properties of non-linear computational mappings in an attempt to include the whole physical space and avoid leaving the computational space. We have seen that the mapping of a high dimensional Hilbert-space onto a two-level system over which operator equivalence is demanded, is a goal that is hard to achieve. The computational interpretation is constrained, as it must keep the linearity of both physical and computational spaces, resulting in a search for specific operators that might fulfill the requirements for operator equivalence. The fact that our physical operators are constructed from permutations of spins and single-spin rotations limits us in the choice of such candidates and increases the complexity needed from our system (system size). We deduce from our attempts that such a scheme is unfavorable (if not impossible). However,

as we will see in Chapter 5, one can attempt operations that take the qubit out of the computational space. With a projection of the qubit back to the computational space, a CNOT operation is performed.

## 5 CNOT on a singlet-triplet basis

Our goal in this chapter is the same as in the previous chapter. We search for physical operators that will enable us to implement universal quantum computation over a multi-spin qubit. We target the universal set of gates:

$$G = \{\{\text{single qubit gates}\}, \text{CNOT}\}. \quad (5.1)$$

We assume that the single-qubit gates are already implemented and focus on implementing the Controlled-NOT (CNOT) gate that entangles two qubits:

$$\text{CNOT} = \begin{pmatrix} 1 & 0 & 0 & 0 \\ 0 & 1 & 0 & 0 \\ 0 & 0 & 0 & 1 \\ 0 & 0 & 1 & 0 \end{pmatrix}. \quad (5.2)$$

We now take a different approach from the one in Chapter 4 and focus on a specific two-spin physical system where the qubit encoding is set to the singlet-triplet (S-T) non-degenerate system. In this case, the computational mapping  $f : \mathcal{H}_4 \rightarrow \mathcal{H}_2^{\text{comp}}$  projects away two dimensions from the physical state and is linear on the remaining states:

$$f(|\psi\rangle_2) := \begin{cases} 0 & \text{if } |\psi\rangle_2 \in \ker(f) = \text{span}\{|\uparrow\uparrow\rangle, |\downarrow\downarrow\rangle\}, \\ |0\rangle & \text{if } |\psi\rangle_2 = |T\rangle = \frac{|\uparrow\downarrow\rangle + |\downarrow\uparrow\rangle}{\sqrt{2}}, \\ |1\rangle & \text{if } |\psi\rangle_2 = |S\rangle = \frac{|\uparrow\downarrow\rangle - |\downarrow\uparrow\rangle}{\sqrt{2}}. \end{cases} \quad (5.3)$$

Thus, we avoid the non-linear computational mapping problems presented in Section 4.3.

Now that we have defined our system, we write the requested result of the CNOT gate on this S-T qubit. Let  $|\psi\rangle$  be a general state of control and target qubits. The result of the CNOT gate is the following:

$$\begin{aligned} C\hat{N}OT(|\psi\rangle) &= C\hat{N}OT(|\psi\rangle_c \otimes |\psi\rangle_t) \\ &= C\hat{N}OT([\alpha|T\rangle_c + \beta|S\rangle_c] \otimes [\gamma|T\rangle_t + \delta|S\rangle_t]) \\ &= C\hat{N}OT(\alpha\gamma|T\rangle_c|T\rangle_t + \alpha\delta|T\rangle_c|S\rangle_t + \beta\gamma|S\rangle_c|T\rangle_t + \beta\delta|S\rangle_c|S\rangle_t) \\ &= \alpha\gamma|T\rangle_c|T\rangle_t + \alpha\delta|T\rangle_c|S\rangle_t + \beta\gamma|S\rangle_c|S\rangle_t + \beta\delta|S\rangle_c|T\rangle_t. \end{aligned} \quad (5.4)$$

In other words, on the target state  $|\psi_t\rangle$ , a NOT operation is performed only for the part where the control state  $|\psi_c\rangle$  is equal to  $|1\rangle = |S\rangle$ .

We saw in Chapter 4 that in a qubit system of this type, many operations send the qubit state out of the computational space. However, to loosen our constraints, we allow such operations on our qubits as long as the qubit returns to the computational space at the end of some operator sequence. Furthermore, we do not restrict ourselves to spin-braiding as physical operations and look for other feasible physical operations that will help us in the CNOT gate implementation, e.g. spin parity operation using charge detection as proposed in Ref. [26]. We wish to use spin-braiding as part of the entangling procedure between two qubits by the exchange of spins between them (as shown in Fig. 5).

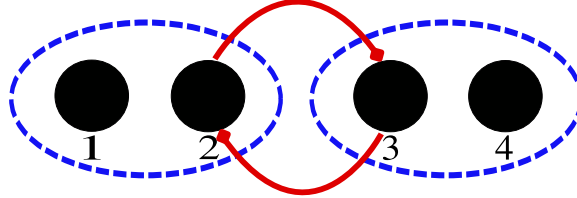


Figure 5: Exchange of spins between two singlet-triplet qubits as a mean to cause entanglement.

In Section 5.1 we present a classical CNOT gate and study the effects of leaving the computational space and returning to it. In Section 5.2 we present a quantum CNOT gate over this S-T qubit.

### 5.1 A classical CNOT

We present here the effects of spin-braiding on S-T qubits. When we swap spins 2 and 3 between the qubits we break out of the computational space. We use a *spin parity measurement* to project the four-spin state back to the two-qubit space and realize that a classical CNOT gate is achieved by the measurement of the control qubit.

Let  $|\psi\rangle$  be a state of the two non-entangled qubits. This state can be decomposed into the tensor product of the two qubits states, which in turn can be written in the S-T basis:

$$\begin{aligned} |\psi\rangle &= |\psi\rangle_c \otimes |\psi\rangle_t = [\alpha |T\rangle + \beta |S\rangle]_c \otimes [\gamma |T\rangle + \delta |S\rangle]_t \\ &= \alpha\gamma |T\rangle_c |T\rangle_t + \alpha\delta |T\rangle_c |S\rangle_t + \beta\gamma |S\rangle_c |T\rangle_t + \beta\delta |S\rangle_c |S\rangle_t. \end{aligned} \tag{5.5}$$

### 5.1.1 Spin-braiding between the qubits

In order to understand the operation of the spin-braiding between the qubits we write  $|\psi\rangle$  over the normal spin-basis:

$$\begin{aligned}
 |\psi\rangle &= \frac{\alpha\gamma}{2} (|\uparrow\downarrow\rangle_c |\uparrow\downarrow\rangle_t + |\downarrow\uparrow\rangle_c |\uparrow\downarrow\rangle_t + |\uparrow\downarrow\rangle_c |\downarrow\uparrow\rangle_t + |\downarrow\uparrow\rangle_c |\downarrow\uparrow\rangle_t) \\
 &+ \frac{\alpha\delta}{2} (|\uparrow\downarrow\rangle_c |\uparrow\downarrow\rangle_t + |\downarrow\uparrow\rangle_c |\uparrow\downarrow\rangle_t - |\uparrow\downarrow\rangle_c |\downarrow\uparrow\rangle_t - |\downarrow\uparrow\rangle_c |\downarrow\uparrow\rangle_t) \\
 &+ \frac{\beta\gamma}{2} (|\uparrow\downarrow\rangle_c |\uparrow\downarrow\rangle_t - |\downarrow\uparrow\rangle_c |\uparrow\downarrow\rangle_t + |\uparrow\downarrow\rangle_c |\downarrow\uparrow\rangle_t - |\downarrow\uparrow\rangle_c |\downarrow\uparrow\rangle_t) \\
 &+ \frac{\beta\delta}{2} (|\uparrow\downarrow\rangle_c |\uparrow\downarrow\rangle_t - |\downarrow\uparrow\rangle_c |\uparrow\downarrow\rangle_t - |\uparrow\downarrow\rangle_c |\downarrow\uparrow\rangle_t + |\downarrow\uparrow\rangle_c |\downarrow\uparrow\rangle_t).
 \end{aligned} \tag{5.6}$$

Let  $\hat{B}_2$  be the operator swapping two spins between the qubits, i.e. spins 2 and 3 in Fig. 5. The swap operator applied to  $|\psi\rangle$  results in  $|\tilde{\psi}\rangle = \hat{B}_2 |\psi\rangle$  which is the following (we ignore the overall fermionic statistic):

$$\begin{aligned}
 |\tilde{\psi}\rangle &= \frac{\alpha\gamma}{2} (|\uparrow\uparrow\rangle_c |\downarrow\downarrow\rangle_t + |\downarrow\uparrow\rangle_c |\uparrow\downarrow\rangle_t + |\uparrow\downarrow\rangle_c |\downarrow\uparrow\rangle_t + |\downarrow\downarrow\rangle_c |\uparrow\uparrow\rangle_t) \\
 &+ \frac{\alpha\delta}{2} (|\uparrow\uparrow\rangle_c |\downarrow\downarrow\rangle_t + |\downarrow\uparrow\rangle_c |\uparrow\downarrow\rangle_t - |\uparrow\downarrow\rangle_c |\downarrow\uparrow\rangle_t - |\downarrow\downarrow\rangle_c |\uparrow\uparrow\rangle_t) \\
 &+ \frac{\beta\gamma}{2} (|\uparrow\uparrow\rangle_c |\downarrow\downarrow\rangle_t - |\downarrow\uparrow\rangle_c |\uparrow\downarrow\rangle_t + |\uparrow\downarrow\rangle_c |\downarrow\uparrow\rangle_t - |\downarrow\downarrow\rangle_c |\uparrow\uparrow\rangle_t) \\
 &+ \frac{\beta\delta}{2} (|\uparrow\uparrow\rangle_c |\downarrow\downarrow\rangle_t - |\downarrow\uparrow\rangle_c |\uparrow\downarrow\rangle_t - |\uparrow\downarrow\rangle_c |\downarrow\uparrow\rangle_t + |\downarrow\downarrow\rangle_c |\uparrow\uparrow\rangle_t).
 \end{aligned} \tag{5.7}$$

The result of the swapping is presented in Fig. 6. The new state can be decomposed into a product state of the previous qubit states (as shown by the solid lines). However, a decomposition into a product of the qubit states (two left spins times the two right ones as shown by the dashed lines) is impossible. Furthermore, the new state is partially out of the computational space of the qubit encoding, i.e. this state cannot be fully decomposed in the  $|S\rangle, |T\rangle$  basis.

### 5.1.2 Projection back to the computational space

In order to project the qubits back to the computational space, a destructive measurement must be applied that projects the spin building blocks to their new qubit encoding. This must involve some two-spin measurement operator. Thus, we expand the operator group  $B$  from the previous chapter and introduce operators which are not spin-braiding.

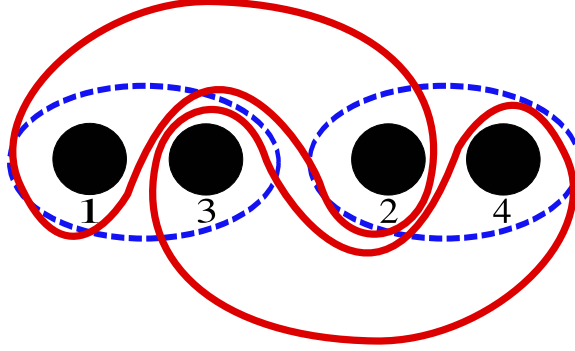


Figure 6: After the swap of spins between the singlet-triplet qubits, we are left with an entangled state under the division into two qubits (dashed circles). The qubits are highly entangled as the state of the previous qubits remain unaffected (solid line shapes). A spin-swap like this takes the new qubits state out of the computational space and a measurement of the new qubits must project the qubits back to it, e.g. a parity measurement of the first qubit, i.e. of spins 1 and 3.

We choose to use a *spin parity measurement* on the first qubit's spins to demonstrate that the two qubits can be projected back to the computational space. In this spin parity measurement we measure whether the two spins of the qubit are aligned (even parity) or not (odd parity). This measurement can be achieved by a charge measurement as proposed in Ref. [26]. Such a charge measurement requires the spins to be in the same double quantum dot and is a local property of this double-dot. In our qubit interpretation such a double-dot is equivalent to our qubit. Thus, such a charge measurement will be a local qubit operation.

Let  $\hat{P}_{1,2}$  be the operator that measures the spin parity of the spins in the left qubit of  $|\tilde{\psi}\rangle$ . The result  $|\psi_{\{p\}}\rangle = \hat{P}_{1,2} |\tilde{\psi}\rangle$  depends on the outcome of the measurement, i.e.  $p = 1$  is even parity and  $p = 0$  is odd parity and is the

following:

$$|\psi_{\{0\}}\rangle = \rho_0 \left[ \frac{\alpha\gamma}{\sqrt{2}} (|\downarrow\uparrow\rangle_c |\uparrow\downarrow\rangle_t + |\uparrow\downarrow\rangle_c |\downarrow\uparrow\rangle_t) + \frac{\alpha\delta}{\sqrt{2}} (|\downarrow\uparrow\rangle_c |\uparrow\downarrow\rangle_t - |\uparrow\downarrow\rangle_c |\downarrow\uparrow\rangle_t) - \frac{\beta\gamma}{\sqrt{2}} (|\downarrow\uparrow\rangle_c |\uparrow\downarrow\rangle_t - |\uparrow\downarrow\rangle_c |\downarrow\uparrow\rangle_t) - \frac{\beta\delta}{\sqrt{2}} (|\downarrow\uparrow\rangle_c |\uparrow\downarrow\rangle_t + |\uparrow\downarrow\rangle_c |\downarrow\uparrow\rangle_t) \right], \quad (5.8)$$

$$|\psi_{\{1\}}\rangle = \rho_1 \left[ \frac{\alpha\gamma}{\sqrt{2}} (|\uparrow\uparrow\rangle_c |\downarrow\downarrow\rangle_t + |\downarrow\downarrow\rangle_c |\uparrow\uparrow\rangle_t) + \frac{\alpha\delta}{\sqrt{2}} (|\uparrow\uparrow\rangle_c |\downarrow\downarrow\rangle_t - |\downarrow\downarrow\rangle_c |\uparrow\uparrow\rangle_t) + \frac{\beta\gamma}{\sqrt{2}} (|\uparrow\uparrow\rangle_c |\downarrow\downarrow\rangle_t - |\downarrow\downarrow\rangle_c |\uparrow\uparrow\rangle_t) + \frac{\beta\delta}{\sqrt{2}} (|\uparrow\uparrow\rangle_c |\downarrow\downarrow\rangle_t + |\downarrow\downarrow\rangle_c |\uparrow\uparrow\rangle_t) \right], \quad (5.9)$$

where  $\rho_0, \rho_1$  are normalization factors.

We note that in the even-parity case,  $p = 1$ , we are left with a state which is completely out of the computational space. However, when even parity is measured, we can flip the spins 1 and 3 and obtain a similar result to the odd-parity case (identical up to a sign of the coefficients).

We denote this conditional flip operation  $\hat{F}_{1,3}^c$  and its application on the state results in  $|\tilde{\psi}_{\{p\}}\rangle = \hat{F}_{1,3}^c |\psi_{\{p\}}\rangle$  which is:

$$|\tilde{\psi}_{\{0\}}\rangle = |\psi_{\{0\}}\rangle, \quad (5.10)$$

$$|\tilde{\psi}_{\{1\}}\rangle = \rho_1 \left[ \frac{\alpha\gamma}{\sqrt{2}} (|\downarrow\uparrow\rangle_c |\uparrow\downarrow\rangle_t + |\uparrow\downarrow\rangle_c |\downarrow\uparrow\rangle_t) + \frac{\alpha\delta}{\sqrt{2}} (|\downarrow\uparrow\rangle_c |\uparrow\downarrow\rangle_t - |\uparrow\downarrow\rangle_c |\downarrow\uparrow\rangle_t) + \frac{\beta\gamma}{\sqrt{2}} (|\downarrow\uparrow\rangle_c |\uparrow\downarrow\rangle_t - |\uparrow\downarrow\rangle_c |\downarrow\uparrow\rangle_t) + \frac{\beta\delta}{\sqrt{2}} (|\downarrow\uparrow\rangle_c |\uparrow\downarrow\rangle_t + |\uparrow\downarrow\rangle_c |\downarrow\uparrow\rangle_t) \right]. \quad (5.11)$$

Thus, we obtain a state which is an entangled state of the two-qubits. This state is fully within the computational space and we can decompose it in the S-T computational basis of each qubit using the following relations:

$$|\uparrow\downarrow\rangle = \frac{1}{\sqrt{2}} (|T\rangle + |S\rangle), \quad (5.12)$$

$$|\downarrow\uparrow\rangle = \frac{1}{\sqrt{2}} (|T\rangle - |S\rangle). \quad (5.13)$$

However, the parity measurement has projected the system onto a state where we have lost information about the original qubit states. The state we obtain is the following:

$$|\tilde{\psi}_{\{p\}}\rangle = \rho_p [(\alpha\gamma + (-1)^{p+1}\beta\delta) [ |T\rangle_c |T\rangle_t - |S\rangle_c |S\rangle_t ] + (\alpha\delta + (-1)^{p+1}\beta\gamma) [ |T\rangle_c |S\rangle_t - |S\rangle_c |T\rangle_t ]], \quad (5.14)$$

which is composed of a sum of only two states and not four as was the original control-target state. Thus, no operation will enable us to achieve the result of the CNOT gate from this state.

### 5.1.3 A classical CNOT can be obtained

The state  $|\tilde{\psi}_{\{p\}}\rangle$  is an entangled state of the two qubits. We notice that if we measure the control qubit ( $\hat{M}_c$ ) in a singlet or a triplet state (i.e.  $z = 1$  or  $z = 0$  respectively), the result  $|\tilde{\psi}_{\{p,z\}}\rangle = \hat{M}_c |\tilde{\psi}_{\{p\}}\rangle$  would be:

$$|\tilde{\psi}_{\{p,1\}}\rangle = -\tilde{\rho}_p |S\rangle_c [(\alpha\gamma + (-1)^{p+1}\beta\delta) |S\rangle_t + (\alpha\delta + (-1)^{p+1}\beta\gamma) |T\rangle_t], \quad (5.15)$$

$$|\tilde{\psi}_{\{p,0\}}\rangle = \tilde{\rho}_p |T\rangle_c [(\alpha\gamma + (-1)^{p+1}\beta\delta) |T\rangle_t + (\alpha\delta + (-1)^{p+1}\beta\gamma) |S\rangle_t], \quad (5.16)$$

where  $\tilde{\rho}_p$  are normalization factors.

If a singlet is measured ( $z = 1$ ) we rotate the target qubit with a  $\hat{\sigma}_x$  operation and obtain the same result as in the case that a triplet is measured (up to a global phase)

$$|\tilde{\psi}_{\{p,z\}}\rangle = (-1)^z \tilde{\rho}_1 |z\rangle_c [(\alpha\gamma + (-1)^{p+1}\beta\delta) |T\rangle_t + (\alpha\delta + (-1)^{p+1}\beta\gamma) |S\rangle_t]. \quad (5.17)$$

From this state it is easy to see that once the control qubit is in a pure computational state we obtain the result of a classical CNOT gate in the target qubit (up to a global phase), i.e.

$$|\psi\rangle_c = |T\rangle \Rightarrow |\tilde{\psi}_{\{p,z\}}\rangle = (-1)^z |z\rangle_c [\gamma |T\rangle_t + \delta |S\rangle_t], \quad (5.18)$$

$$|\psi\rangle_c = |S\rangle \Rightarrow |\tilde{\psi}_{\{p,z\}}\rangle = (-1)^{z+p+1} |z\rangle_c [\delta |T\rangle_t + \gamma |S\rangle_t]. \quad (5.19)$$

However, this is a classical process as the state of the control qubit is in a pure state and its information is destroyed by the measurement. Thus, this gate cannot be used to entangle the two qubits.

### 5.1.4 Summary

We have seen that after the swapping of spins between S-T qubits we obtain a state which is entangled but also has parts which are outside of the computational space. We have suggested a series of measurements that project the

state back on the computational space, which results in a classical-CNOT gate. However, a classical-CNOT gate means that the qubits are no longer entangled at the end of the procedure. Therefore, we propose a different scheme in Section 5.2 in order to achieve a quantum CNOT gate.

We note that all the operations except the spin swap have been local qubit operations (including the parity measurement). The spin-swap is non-local with respect to the qubits, but involves only two neighboring spins and, thus, is local.

## 5.2 CNOT using spin parity measurements

We wish to perform a CNOT operation over the singlet-triplet (S-T) qubits. So far, we have managed to construct a classical CNOT operation using spin-swap and a spin parity measurement. We are encouraged by this result and set out to construct a S-T parity measurement using the same set of operations (Section 5.2.1). From there, we expand the result from Ref. [27], where spin parity is used as a means to implement a CNOT on a pair of single-spin qubits. Thus, we use the S-T parity as the means for the S-T CNOT implementation (Section 5.2.2).

### 5.2.1 Equivalence between spin parity and singlet-triplet parity

We present here a method for measuring the S-T parity between two qubits by measuring the spin parity within one of the two-spin qubits. In our scheme, a S-T parity is a non-local two-qubit projective operation. Let  $|\psi\rangle$  be a general two S-T qubit state. The S-T parity measurement  $\hat{P}$  results in:

$$\begin{aligned} \hat{P}(|\psi\rangle) &= \hat{P}([\alpha |T\rangle_1 + \beta |S\rangle_1] \otimes [\gamma |T\rangle_2 + \delta |S\rangle_2]) \\ &= \begin{cases} \rho_1 [\alpha\gamma |T\rangle_1 |T\rangle_2 + \beta\delta |S\rangle_1 |S\rangle_2] & \text{if } p = 1, \\ \rho_0 [\alpha\delta |T\rangle_1 |S\rangle_2 + \beta\gamma |S\rangle_1 |T\rangle_2] & \text{if } p = 0. \end{cases} \end{aligned} \quad (5.20)$$

where  $\rho_p$  are normalization factors.

In order to implement  $\hat{P}$  using spin parity we first define the S-T Hadamard gate. This gate has in the S-T basis  $\{|T\rangle, |S\rangle\}$  the following matrix representation:

$$\hat{H} \equiv \frac{1}{\sqrt{2}} \begin{bmatrix} 1 & 1 \\ 1 & -1 \end{bmatrix}. \quad (5.21)$$

Hence, we note that the S-T basis states, once rotated by S-T Hadamard gates, are of the form:

$$\hat{H}|T\rangle = |\uparrow\downarrow\rangle, \quad (5.22)$$

$$\hat{H}|S\rangle = |\downarrow\uparrow\rangle. \quad (5.23)$$

We see that the left spin of the rotated qubit states can serve as a witness for the original two-spin state, e.g. if the left spin is  $\uparrow$  the original pre-rotated state was a triplet. Hence, the spin parity of the left spin in each rotated qubit (spins 1 and 3) can indicate the parity of the qubits. Thus, all we need to do is to Hadamard-rotate the qubits, measure the spin parity of the left spins, and rotate them back again to their original basis representation. The S-T parity gate is shown in Fig. 7. It can be written in the form:

$$\hat{P} = \hat{H}_1\hat{H}_2\hat{P}_s\hat{H}_1\hat{H}_2, \quad (5.24)$$

where  $\hat{H}_1, \hat{H}_2$  are the Hadamard gates operating on qubits 1 and 2, and  $\hat{P}_s$  is the spin parity measurement of spins 1 and 3.

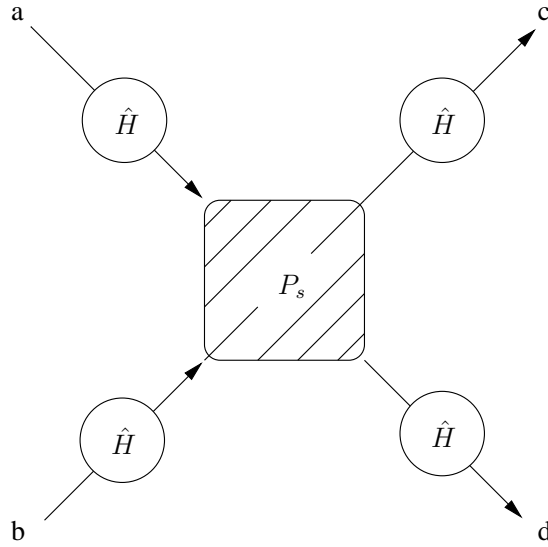


Figure 7: Gate that uses a spin parity measurement to measure the parity of the S-T qubits. A pair of S-T qubits enters the gate in arms  $a$  and  $b$ . Each of the qubits is rotated by a Hadamard gate  $\hat{H}$ . The spin parity of the left spin from each qubit (of spins 1 and 3) is then measured. The qubits are rotated back by Hadamard gates and the parity of the spins is equivalent to the parity of the qubits.

The proposed spin parity measurement in Ref. [26] is local and cannot be carried out over distant spins. Hence, we add spin-swapping to the spin parity operator  $\hat{P}_s$  definition. We swap spins 2 and 3 between the qubits and measure the spin parity of the left qubit. This is exactly the route we have taken in Section 5.1. However, instead of measuring the left qubit's state and reaching a classical CNOT, we swap spins 2 and 3 once more and manage to measure the spin parity of spins 1 and 3 locally. Thus, the operator  $\hat{P}_s$  takes the form:

$$\hat{P}_s = \hat{B}_2 \hat{P}_{1,2} \hat{B}_2, \quad (5.25)$$

where  $\hat{B}_2$  is the swap of spins 2 and 3, and  $\hat{P}_{1,2}$  is the local spin parity measurement achieved by charge detection.

As an example for the S-T parity measurement we show that it can be used to encode a qubit  $|T\rangle$  as the two qubit state  $|T\rangle_1 |T\rangle_2$  and  $|S\rangle$  as the two-qubit state  $|S\rangle_1 |S\rangle_2$  in appendix A.

### 5.2.2 The CNOT gate

We can use this S-T parity measurement to construct a CNOT gate similar to the one presented in Ref. [27]. However, we can take advantage of the availability of Hadamard rotations in our S-T parity measurements to create a simpler gate, presented in Fig. 8.

The main differences between our CNOT and the one in Ref. [27] are:

- All single qubit operations are performed under the S-T qubit computational mapping.
- Our CNOT gate has three Hadamard gates instead of the four Hadamard gates in Ref. [27].
- The ancilla is prepared in a pure computational state (triplet) instead of a superposition of computational states.

The parity and ancilla measurements are projective non-linear operations. Each measurement projects the state into one of two possible outcome states. We present the calculation tree of the CNOT gate in Fig. 9 where the three consecutive measurements leave us with eight possible outcome states.

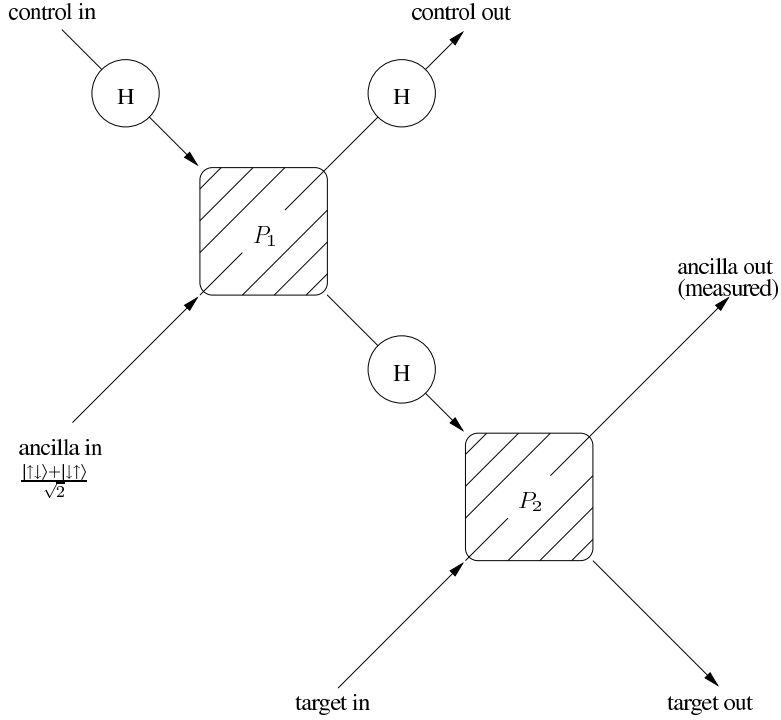


Figure 8: Deterministic CNOT gate for S-T qubits. The boxes represent spin parity measurements of the left spins in each qubit as described in Eq. (5.25). Three Hadamard gates rotate the qubits entering and leaving the first box. The input of the CNOT gate consists of a control and target qubit plus an ancilla prepared in a triplet state. The ancilla is measured at the output in a singlet or a triplet state. The outcome of this measurement plus the two parities measured, determine which operators  $\sigma_c, \sigma_t$  one has to apply on the control and target qubits in order to complete the CNOT operation. In appendix B we find that for the control qubit the following is applied  $\sigma_c = \sigma_z$  if  $p_2 = 0$  and  $\sigma_c = 1$  if  $p_2 = 1$ . For the target qubit,  $\sigma_t = \sigma_x$  if  $p_1 = 1$  and the ancilla is measured in  $|S\rangle$  state, or if  $p_1 = 0$  and the ancilla is measured in  $|T\rangle$  state. Otherwise,  $\sigma_t = 1$ .

However, as seen in the figure, the last tuning step of the gate leads to a single deterministic result.

In appendix B, we find the needed tuning operators and prove that our gate, in Fig. 8, is equivalent to a CNOT gate. We first calculate the gate's operation on the computational pure basis states in order to find the tuning operation (appendix B.1). Afterwards, we prove that the gate is linear

(appendix B.2). This is done by following the calculation tree of Fig. 9 when the gate is applied to an arbitrary two-qubit state.

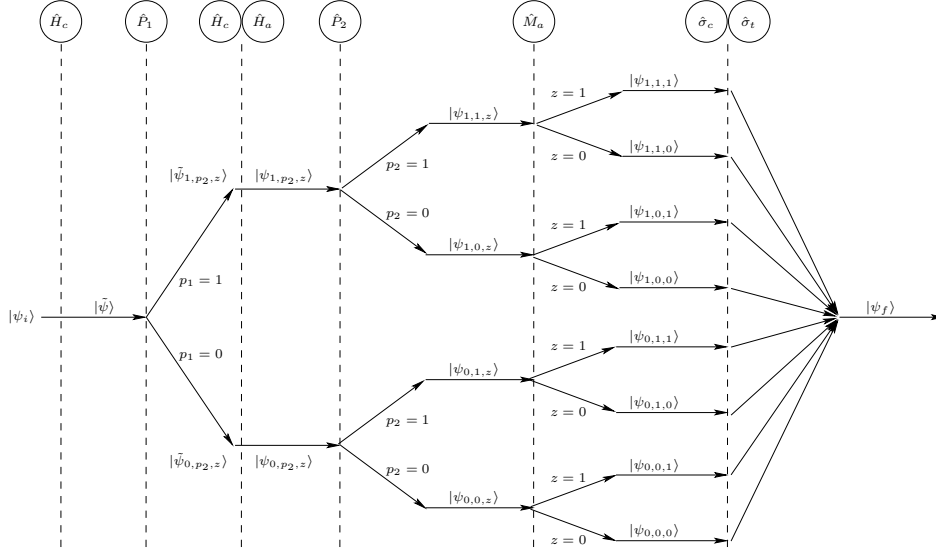


Figure 9: The computation tree of the spin parity CNOT gate. The computation splits in accordance with the parity and ancilla measurements. Due to the Hadamard gate rotations, the measurements do not destroy the initial state. Thus, each path of the computation has the same probability of occurring. We obtain eight possible result states which we denote as  $|\psi_{p_1,p_2,z}\rangle$ . We follow the gate's execution and show that the result in each of the calculation arms merges into one result  $|\psi_f\rangle$  which is equal to the result of the CNOT operation. The calculation of this computation tree is presented in Appendix B.2.

### 5.2.3 Summary

We have used a local charge measurement as a deterministic spin parity measurement on the spins of a S-T qubit. With the use of spin-swapping we could measure the spin parity of spins from different qubits. Thus, we could implement a S-T parity measurement for our qubits. Using this, we constructed a CNOT gate on our qubits. The CNOT gate is composed of three S-T Hadamard gate rotations, two spin parity measurements, an ancilla, and single-qubit gates that tune the final result in relation to the measurement classical results.

### 5.3 Summary

In this chapter we have investigated the necessary execution, beyond mere spin-braiding, for the implementation of a CNOT gate on a S-T qubit system. We introduced a local charge measurement as a means to measure spin parity on a qubit and allowed a spin-braiding to take us out of the computational space. We presented a scheme where the spin parity measurement destroyed our state, enabling us only to produce a classical CNOT gate. Thereafter, we expanded this scheme and found equivalence between a spin parity measurement and a S-T qubit parity. Thus, we could use this result to produce the CNOT gate depicted in Fig. 8.

## 6 Summary

We present here a summary of the achievements of this thesis. We provide an overview of the results of this research and an outlook for future study in this direction.

### 6.1 Overview

This thesis presents a systematic definition of the mathematical language required for addressing multi-particle qubits. Even though the problem of implementing a qubit is of a physical nature, this language enabled us to address general attributes and approaches for such physical implementations.

We have defined a non-linear computational mapping function that describes the way we interpret a physical system as a qubit. We could categorize three families of such mappings: Projection on a two-level system, partial projection, and no projection at all.

The latter two families describe multi-dimensional computational spaces and are rarely studied. We described the guidelines one must follow in using such mappings and presented examples where the complexity of such mappings is demonstrated by failing to implement universal quantum computation using these schemes.

During this study we found local physical operations that can be used for computation on multi-particle qubits. When we limited ourselves to computational mappings of the *Projection on a two-level system* type, we could implement a CNOT gate on a S-T qubit system using these operations. This is a stepping stone for this type of system as the CNOT gate is implemented by local non-interacting physical operations and offers a deterministic coherent implementation.

### 6.2 Outlook

Our mathematical approach for the multi-particle qubit question has introduced a language that can and should be used in order to understand the relationship between the physical and logical aspects of qubits. We have studied a single type of multi-particle qubits that is composed of spins-1/2. Many other systems can be studied under our mathematical definitions.

The non-linear properties of the computational mappings will probably unfold in the future as more scientists turn to study the field of non-linear algebra. We have presented the problem and an intuitive physical approach that can be expanded with further mathematical research.

We could not study systems composed of a large number of spins. The Hilbert space dimension grows exponentially with spin number and the computation of operator equivalence is long. As computation power will increase one could use our approach and algorithms to address larger systems of multi-particle qubits and find suitable physical operations for universal quantum computation.

From a physical point of view, throughout the thesis, we used the operation of swapping the spins locations in order to achieve quantum gates. Such operations have yet to be implemented. The CNOT scheme we present can encourage experiments that will implement such swap operations and produce our proposed CNOT gate for S-T qubits.

## 7 Acknowledgments

I would like to thank Prof. Dr. Daniel Loss for proposing this research topic to me. He gave me this opportunity to step into the quantum computation world, to work in his group, and shared his ideas and experience with me. A special thank to Dr. Bernd Braunecker, that guided me all along this work with a lot of patience and insight. And to, Prof. Dr. Guido Burkard, Dr. Dimitrije Stepanenko, Dr. Otfried Guehne, and Luca Chirolli for fruitful discussions. Also to Dr. Bill Coish and Markus Mangold that have had the patience to read this thesis and remark it. Thanks.

## A Singlet-triplet parity encoder

The S-T parity measurement  $\hat{P}$  can be used to encode a qubit  $|T\rangle$  as the two qubit state  $|T\rangle_1 |T\rangle_2$  and  $|S\rangle$  as the two qubit state  $|S\rangle_1 |S\rangle_2$ . We use the proof of this claim in order to present the operation of the gate.

Let  $|\psi\rangle_1$  be the qubit that is to be encoded and the second qubit be an ancilla prepared in the state  $|\uparrow\downarrow\rangle$ . We can decompose the first qubit in the S-T basis,

$$|\psi_1\rangle = |\psi\rangle_1 |\uparrow\downarrow\rangle_2 = (\alpha |T\rangle_1 + \beta |S\rangle_1) |\uparrow\downarrow\rangle_2. \quad (\text{A.1})$$

The qubits pass through the first S-T Hadamard gates:

$$|\psi_2\rangle = \hat{H}_1 \hat{H}_2 |\psi_1\rangle = (\alpha |\uparrow\downarrow\rangle_1 + \beta |\downarrow\uparrow\rangle_1) \left( \frac{|\uparrow\downarrow\rangle_2 + |\downarrow\uparrow\rangle_2}{\sqrt{2}} \right). \quad (\text{A.2})$$

In order to locally measure the parity of spins 1 and 3, we swap spins 2 and 3 between the qubits:

$$\begin{aligned} |\psi_3\rangle = \hat{B}_2 |\psi_2\rangle = & \frac{\alpha}{\sqrt{2}} (|\uparrow\uparrow\rangle_1 |\downarrow\downarrow\rangle_2 + |\uparrow\downarrow\rangle_1 |\downarrow\uparrow\rangle_2) + \\ & \frac{\beta}{\sqrt{2}} (|\downarrow\downarrow\rangle_1 |\uparrow\uparrow\rangle_2 + |\downarrow\uparrow\rangle_1 |\uparrow\downarrow\rangle_2). \end{aligned} \quad (\text{A.3})$$

The result of the spin parity measurement  $\hat{P}_{1,2}$  is:

$$|\psi_4, p\rangle = \hat{P}_{1,2} |\psi_3\rangle = \begin{cases} \alpha |\uparrow\uparrow\rangle_1 |\downarrow\downarrow\rangle_2 + \beta |\downarrow\downarrow\rangle_1 |\uparrow\uparrow\rangle_2 & \text{if } p = 1, \\ \alpha |\uparrow\downarrow\rangle_1 |\downarrow\uparrow\rangle_2 + \beta |\downarrow\uparrow\rangle_1 |\uparrow\downarrow\rangle_2 & \text{if } p = 0. \end{cases} \quad (\text{A.4})$$

The spins are swapped again and return to their original position:

$$|\psi_5, p\rangle = \hat{B}_2 |\psi_4, p\rangle = \begin{cases} \alpha |\uparrow\downarrow\rangle_1 |\uparrow\downarrow\rangle_2 + \beta |\downarrow\uparrow\rangle_1 |\downarrow\uparrow\rangle_2 & \text{if } p = 1, \\ \alpha |\uparrow\uparrow\rangle_1 |\downarrow\downarrow\rangle_2 + \beta |\downarrow\downarrow\rangle_1 |\uparrow\uparrow\rangle_2 & \text{if } p = 0. \end{cases} \quad (\text{A.5})$$

The last step of the S-T operation is to Hadamard-rotate both qubits back to the S-T basis:

$$|\psi_6, p\rangle = \hat{H}_1 \hat{H}_2 |\psi_5, p\rangle = \begin{cases} \alpha |T\rangle_1 |T\rangle_2 + \beta |S\rangle_1 |S\rangle_2 & \text{if } p = 1, \\ \alpha |T\rangle_1 |S\rangle_2 + \beta |S\rangle_1 |T\rangle_2 & \text{if } p = 0. \end{cases} \quad (\text{A.6})$$

Application of a conditional  $\hat{\sigma}_2^p$  operation, where  $\hat{\sigma}_2^p = 1$  if  $p = 1$  and  $\hat{\sigma}_2^p = \hat{\sigma}_x$  if  $p = 0$ , results in the deterministic result of the encoder:

$$|\psi_7\rangle = \hat{\sigma}_2^p |\psi_6, p\rangle = \alpha |T\rangle_1 |T\rangle_2 + \beta |S\rangle_1 |S\rangle_2. \quad (\text{A.7})$$

## B Verification of the CNOT gate operation

We prove here the operation of the CNOT gate presented in Fig. 8. This gate operates on S-T qubits defined by the computational mapping  $f$  from Eq. 5.3. It denotes the triplet state by  $|T\rangle = |0\rangle$  and the singlet by  $|S\rangle = |1\rangle$ .

We calculate the gate's operation over pure computational basis states and find the correction operations needed at the end of the gate's calculation in Section B.1. Thereafter, in Section B.2 we show the calculation for all eight computation arms presented in Fig. 9. We show it for an arbitrary state of the control and target qubits, thus, proving the linearity of the CNOT operation.

### B.1 Proof over pure computational basis states

We prove here the case where the input control  $|x\rangle$  and target  $|y\rangle$  qubits are in a pure computational state  $x, y \in \{0, 1\}$ .

We ignore normalization constants in the following proof and additions are assumed to be modulo 2.

The CNOT operation can be written as:

$$|x\rangle |y\rangle \rightarrow |x\rangle |x + y\rangle. \quad (\text{B.1})$$

The Hadamard operation is written as:

$$|x\rangle \rightarrow |0\rangle + (-1)^x |1\rangle. \quad (\text{B.2})$$

We follow the operation of the gate sequentially. The initial state of the control, target and ancilla qubits is:

$$|\psi_i\rangle = |x\rangle |a\rangle |y\rangle. \quad (\text{B.3})$$

The control qubit is passing through a Hadamard gate. The ancilla is prepared in state  $|a\rangle = |0\rangle$ . At the entrance to the upper spin parity gate the state of the qubits is:

$$|\psi_i\rangle \rightarrow |\tilde{\psi}\rangle = (|0\rangle + (-1)^x |1\rangle) |0\rangle |y\rangle. \quad (\text{B.4})$$

Measuring the spin parity of the left spin from each qubit results in:

$$|\tilde{\psi}\rangle \rightarrow \begin{cases} |\tilde{\psi}_1\rangle = (|0\rangle + (-1)^x |1\rangle)(|0\rangle + (-1)^x |1\rangle) |y\rangle & \text{if } p_1 = 1, \\ |\tilde{\psi}_0\rangle = (|0\rangle + (-1)^x |1\rangle)(|0\rangle + (-1)^{(x+1)} |1\rangle) |y\rangle & \text{if } p_1 = 0. \end{cases} \quad (\text{B.5})$$

---

*B VERIFICATION OF THE CNOT GATE OPERATION*

---

At the exit both qubit are passing through Hadamard gates:

$$\begin{aligned} |\tilde{\psi}_1\rangle &\rightarrow |\psi_1\rangle = |x\rangle |x\rangle |y\rangle & \text{if } p_1 = 1, \\ |\tilde{\psi}_0\rangle &\rightarrow |\psi_0\rangle = |x\rangle |x+1\rangle |y\rangle & \text{if } p_1 = 0, \end{aligned} \quad (\text{B.6})$$

which can be rewritten as:

$$|\psi_{p_1}\rangle = |x\rangle |x+p_1+1\rangle |y\rangle. \quad (\text{B.7})$$

The second ket enters the second spin parity gate with the target qubit:

$$\begin{aligned} |\psi_{p_1}\rangle &\rightarrow |\psi_{p_1,1}\rangle = |x\rangle [(|0\rangle + |1\rangle)_1(|0\rangle + |1\rangle)_2] + (-1)^{(a+y)} |x\rangle [(|0\rangle - |1\rangle)_1(|0\rangle - |1\rangle)_2] \\ &= |x\rangle |0\rangle \left[ |0\rangle + |1\rangle + (-1)^{(a+y)} |0\rangle - (-1)^{(a+y)} |1\rangle \right] + \\ &\quad |x\rangle |1\rangle \left[ |0\rangle + |1\rangle - (-1)^{(a+y)} |0\rangle + (-1)^{(a+y)} |1\rangle \right] \\ &= |x\rangle |0\rangle |a+y\rangle + |x\rangle |1\rangle |a+y+1\rangle & \text{if } p_2 = 1, \end{aligned} \quad (\text{B.8})$$

$$\begin{aligned} |\psi_{p_1}\rangle &\rightarrow |\psi_{p_1,0}\rangle = (-1)^y |x\rangle [(|0\rangle + |1\rangle)_1(|0\rangle - |1\rangle)_2] + (-1)^a |x\rangle [(|0\rangle - |1\rangle)_1(|0\rangle + |1\rangle)_2] \\ &= |x\rangle |0\rangle \left[ (-1)^y |0\rangle - (-1)^y |1\rangle + (-1)^a |0\rangle - (-1)^a |1\rangle \right] + \\ &\quad |x\rangle |1\rangle \left[ (-1)^y |0\rangle - (-1)^y |1\rangle - (-1)^a |0\rangle + (-1)^a |1\rangle \right] \\ &= (-1)^a |x\rangle |0\rangle |a+y\rangle - (-1)^a |x\rangle |1\rangle |a+y+1\rangle & \text{if } p_2 = 0, \end{aligned} \quad (\text{B.9})$$

Substituting  $a = x + p_1 + 1$  into Eqs. (B.8),(B.9) and measuring the ancilla in one of the computational states results in:

$$|\psi_{p_1,p_2,z}\rangle = (-1)^{(p_2+1)(x+z+p_1+1)} |x\rangle |x+y+z+p_1+1\rangle, \quad (\text{B.10})$$

where  $z$  is the result of the measurement of the ancilla qubit.

We compare eqs. (B.10) and (B.1) to find the post-corrections needed to complete the CNOT operation. The phase factor  $(-1)^{(p_2+1)(z+p_1+1)}$  is input independent and is irrelevant. The phase factor  $(-1)^{(p_2+1)x}$  is eliminated by performing a  $\sigma_z$  operation on the control qubit if  $p_2 = 0$ . Otherwise, no operation is required on the control qubit. To transform the state  $|x+y+z+p_1+1\rangle$  to the required  $|x+y\rangle$  a  $\sigma_x$  operation is applied on the target qubit if  $z+p_1 = 0$ . If  $z+p_1 = 1$ , no operation is needed for the target qubit.

After performing the deterministic post-correction operations our gate's result is equal to the CNOT operation.

## B.2 Proof of linearity

To prove the linearity of the gate that is shown in Fig. 8 we take the control and target qubits to be in arbitrary states:

$$|c\rangle = \alpha |0\rangle + \beta |1\rangle = \alpha |T\rangle + \beta |S\rangle, \quad (\text{B.11})$$

$$|t\rangle = \gamma |0\rangle + \delta |1\rangle = \gamma |T\rangle + \delta |S\rangle. \quad (\text{B.12})$$

Hence, the initial state of the input qubits plus the ancilla is:

$$|\psi_i\rangle = |c\rangle \otimes |a\rangle \otimes |t\rangle = [\alpha |T\rangle_c + \beta |S\rangle_c] \otimes |T\rangle_a \otimes [\gamma |T\rangle_t + \delta |S\rangle_t]. \quad (\text{B.13})$$

The calculation splits in accordance to the parity and ancilla measurements. We obtain eight optional result states which we denote as  $|\psi_{p_1, p_2, z}\rangle$ . We follow the gate's execution as seen in Fig. 9. We prove that the result in each of the calculation arms merges into one result  $|\psi_f\rangle$  which is equal to the result of the CNOT operation.

The control is passing through a S-T Hadamard gate:

$$|\tilde{\psi}\rangle = [\alpha(|T\rangle_c + |S\rangle_c) + \beta(|T\rangle_c - |S\rangle_c)] \otimes |T\rangle_a \otimes [\gamma |T\rangle_t + \delta |S\rangle_t]. \quad (\text{B.14})$$

The first parity measurement is on the control and ancilla qubits. To understand the operation of the spin parity we first write them in the normal spin basis:

$$|\tilde{\psi}\rangle = [\alpha |\uparrow\downarrow\rangle_c + \beta |\downarrow\uparrow\rangle_c] \otimes \frac{|\uparrow\downarrow\rangle_a + |\downarrow\uparrow\rangle_a}{\sqrt{2}} \otimes [\gamma |T\rangle_t + \delta |S\rangle_t]. \quad (\text{B.15})$$

Measuring the spin parity of the first spin of each qubit has two possible results:

$$|\tilde{\psi}_{1, p_2, z}\rangle = [\alpha |\uparrow\downarrow\rangle_c |\uparrow\downarrow\rangle_a + \beta |\downarrow\uparrow\rangle_c |\downarrow\uparrow\rangle_a] \otimes [\gamma |T\rangle_t + \delta |S\rangle_t], \quad (\text{B.16})$$

$$|\tilde{\psi}_{0, p_2, z}\rangle = [\alpha |\uparrow\downarrow\rangle_c |\downarrow\uparrow\rangle_a + \beta |\downarrow\uparrow\rangle_c |\uparrow\downarrow\rangle_a] \otimes [\gamma |T\rangle_t + \delta |S\rangle_t]. \quad (\text{B.17})$$

The ancilla and control qubits are rotated by Hadamard gates:

$$|\psi_{1, p_2, z}\rangle = [\alpha |T\rangle_c |T\rangle_a + \beta |S\rangle_c |S\rangle_a] \otimes [\gamma |T\rangle_t + \delta |S\rangle_t], \quad (\text{B.18})$$

$$|\psi_{0, p_2, z}\rangle = [\alpha |T\rangle_c |S\rangle_a + \beta |S\rangle_c |T\rangle_a] \otimes [\gamma |T\rangle_t + \delta |S\rangle_t]. \quad (\text{B.19})$$

---

*B VERIFICATION OF THE CNOT GATE OPERATION*

---

Now, the ancilla and target qubits enter a spin parity measurement. Once more we write their states in the normal spin basis:

$$|\psi_{1,p_2,z}\rangle = \left[ \alpha |T\rangle_c \frac{|\uparrow\downarrow\rangle_a + |\downarrow\uparrow\rangle_a}{\sqrt{2}} + \beta |S\rangle_c \frac{|\uparrow\downarrow\rangle_a - |\downarrow\uparrow\rangle_a}{\sqrt{2}} \right] \otimes \left[ \gamma \frac{|\uparrow\downarrow\rangle_t + |\downarrow\uparrow\rangle_t}{\sqrt{2}} + \delta \frac{|\uparrow\downarrow\rangle_t - |\downarrow\uparrow\rangle_t}{\sqrt{2}} \right], \quad (\text{B.20})$$

$$|\psi_{0,p_2,z}\rangle = \left[ \alpha |T\rangle_c \frac{|\uparrow\downarrow\rangle_a - |\downarrow\uparrow\rangle_a}{\sqrt{2}} + \beta |S\rangle_c \frac{|\uparrow\downarrow\rangle_a + |\downarrow\uparrow\rangle_a}{\sqrt{2}} \right] \otimes \left[ \gamma \frac{|\uparrow\downarrow\rangle_t + |\downarrow\uparrow\rangle_t}{\sqrt{2}} + \delta \frac{|\uparrow\downarrow\rangle_t - |\downarrow\uparrow\rangle_t}{\sqrt{2}} \right]. \quad (\text{B.21})$$

Measuring the spin parity of the first spin of each qubit splits again the result set in two:

$$|\psi_{1,1,z}\rangle = \frac{\alpha\gamma}{\sqrt{2}} [|T\rangle_c |\uparrow\downarrow\rangle_a |\uparrow\downarrow\rangle_t + |T\rangle_c |\downarrow\uparrow\rangle_a |\downarrow\uparrow\rangle_t] + \frac{\alpha\delta}{\sqrt{2}} [|T\rangle_c |\uparrow\downarrow\rangle_a |\uparrow\downarrow\rangle_t - |T\rangle_c |\downarrow\uparrow\rangle_a |\downarrow\uparrow\rangle_t] + \frac{\beta\gamma}{\sqrt{2}} [|S\rangle_c |\uparrow\downarrow\rangle_a |\uparrow\downarrow\rangle_t - |S\rangle_c |\downarrow\uparrow\rangle_a |\downarrow\uparrow\rangle_t] + \frac{\beta\delta}{\sqrt{2}} [|S\rangle_c |\uparrow\downarrow\rangle_a |\uparrow\downarrow\rangle_t + |S\rangle_c |\downarrow\uparrow\rangle_a |\downarrow\uparrow\rangle_t], \quad (\text{B.22})$$

$$|\psi_{1,0,z}\rangle = \frac{\alpha\gamma}{\sqrt{2}} [|T\rangle_c |\uparrow\downarrow\rangle_a |\downarrow\uparrow\rangle_t + |T\rangle_c |\downarrow\uparrow\rangle_a |\uparrow\downarrow\rangle_t] - \frac{\alpha\delta}{\sqrt{2}} [|T\rangle_c |\uparrow\downarrow\rangle_a |\downarrow\uparrow\rangle_t - |T\rangle_c |\downarrow\uparrow\rangle_a |\uparrow\downarrow\rangle_t] + \frac{\beta\gamma}{\sqrt{2}} [|S\rangle_c |\uparrow\downarrow\rangle_a |\downarrow\uparrow\rangle_t - |S\rangle_c |\downarrow\uparrow\rangle_a |\uparrow\downarrow\rangle_t] - \frac{\beta\delta}{\sqrt{2}} [|S\rangle_c |\uparrow\downarrow\rangle_a |\downarrow\uparrow\rangle_t + |S\rangle_c |\downarrow\uparrow\rangle_a |\uparrow\downarrow\rangle_t], \quad (\text{B.23})$$

$$|\psi_{0,1,z}\rangle = \frac{\alpha\gamma}{\sqrt{2}} [|T\rangle_c |\uparrow\downarrow\rangle_a |\uparrow\downarrow\rangle_t - |T\rangle_c |\downarrow\uparrow\rangle_a |\downarrow\uparrow\rangle_t] + \frac{\alpha\delta}{\sqrt{2}} [|T\rangle_c |\uparrow\downarrow\rangle_a |\uparrow\downarrow\rangle_t + |T\rangle_c |\downarrow\uparrow\rangle_a |\downarrow\uparrow\rangle_t] + \frac{\beta\gamma}{\sqrt{2}} [|S\rangle_c |\uparrow\downarrow\rangle_a |\uparrow\downarrow\rangle_t + |S\rangle_c |\downarrow\uparrow\rangle_a |\downarrow\uparrow\rangle_t] + \frac{\beta\delta}{\sqrt{2}} [|S\rangle_c |\uparrow\downarrow\rangle_a |\uparrow\downarrow\rangle_t - |S\rangle_c |\downarrow\uparrow\rangle_a |\downarrow\uparrow\rangle_t], \quad (\text{B.24})$$

$$\begin{aligned}
 |\psi_{0,0,z}\rangle = & \frac{\alpha\gamma}{\sqrt{2}} [|T\rangle_c |\uparrow\downarrow\rangle_a |\downarrow\uparrow\rangle_t - |T\rangle_c |\downarrow\uparrow\rangle_a |\uparrow\downarrow\rangle_t] - \\
 & \frac{\alpha\delta}{\sqrt{2}} [|T\rangle_c |\uparrow\downarrow\rangle_a |\downarrow\uparrow\rangle_t + |T\rangle_c |\downarrow\uparrow\rangle_a |\uparrow\downarrow\rangle_t] + \\
 & \frac{\beta\gamma}{\sqrt{2}} [|S\rangle_c |\uparrow\downarrow\rangle_a |\downarrow\uparrow\rangle_t + |S\rangle_c |\downarrow\uparrow\rangle_a |\uparrow\downarrow\rangle_t] - \\
 & \frac{\beta\delta}{\sqrt{2}} [|S\rangle_c |\uparrow\downarrow\rangle_a |\downarrow\uparrow\rangle_t - |S\rangle_c |\downarrow\uparrow\rangle_a |\uparrow\downarrow\rangle_t]. \quad (\text{B.25})
 \end{aligned}$$

The ancilla and target qubits can be rewritten over the S-T basis as:

$$\begin{aligned}
 |\uparrow\downarrow\rangle &= \frac{1}{\sqrt{2}} [|T\rangle + |S\rangle], \\
 |\downarrow\uparrow\rangle &= \frac{1}{\sqrt{2}} [|T\rangle - |S\rangle]. \quad (\text{B.26})
 \end{aligned}$$

Substituting Eq. (B.26) in Eq. (B.25) and simplifying the expression we obtain:

$$\begin{aligned}
 |\psi_{1,1,z}\rangle = & \frac{\alpha\gamma}{\sqrt{2}} [|T\rangle_c |T\rangle_a |T\rangle_t + |T\rangle_c |S\rangle_a |S\rangle_t] + \\
 & \frac{\alpha\delta}{\sqrt{2}} [|T\rangle_c |S\rangle_a |T\rangle_t + |T\rangle_c |T\rangle_a |S\rangle_t] + \\
 & \frac{\beta\gamma}{\sqrt{2}} [|S\rangle_c |S\rangle_a |T\rangle_t + |S\rangle_c |T\rangle_a |S\rangle_t] + \\
 & \frac{\beta\delta}{\sqrt{2}} [|S\rangle_c |T\rangle_a |T\rangle_t + |S\rangle_c |S\rangle_a |S\rangle_t], \quad (\text{B.27})
 \end{aligned}$$

$$\begin{aligned}
 |\psi_{1,0,z}\rangle = & \frac{\alpha\gamma}{\sqrt{2}} [|T\rangle_c |T\rangle_a |T\rangle_t - |T\rangle_c |S\rangle_a |S\rangle_t] + \\
 & \frac{\alpha\delta}{\sqrt{2}} [|T\rangle_c |T\rangle_a |S\rangle_t - |T\rangle_c |S\rangle_a |T\rangle_t] + \\
 & \frac{\beta\gamma}{\sqrt{2}} [|S\rangle_c |S\rangle_a |T\rangle_t - |S\rangle_c |T\rangle_a |S\rangle_t] + \\
 & \frac{\beta\delta}{\sqrt{2}} [|S\rangle_c |S\rangle_a |S\rangle_t - |S\rangle_c |T\rangle_a |T\rangle_t], \quad (\text{B.28})
 \end{aligned}$$

$$\begin{aligned}
|\psi_{0,1,z}\rangle &= \frac{\alpha\gamma}{\sqrt{2}} [ |T\rangle_c |S\rangle_a |T\rangle_t + |T\rangle_c |T\rangle_a |S\rangle_t ] + \\
&\quad \frac{\alpha\delta}{\sqrt{2}} [ |T\rangle_c |T\rangle_a |T\rangle_t + |T\rangle_c |S\rangle_a |S\rangle_t ] + \\
&\quad \frac{\beta\gamma}{\sqrt{2}} [ |S\rangle_c |T\rangle_a |T\rangle_t + |S\rangle_c |S\rangle_a |S\rangle_t ] + \\
&\quad \frac{\beta\delta}{\sqrt{2}} [ |S\rangle_c |S\rangle_a |T\rangle_t + |S\rangle_c |T\rangle_a |S\rangle_t ], \tag{B.29}
\end{aligned}$$

$$\begin{aligned}
|\psi_{0,0,z}\rangle &= \frac{\alpha\gamma}{\sqrt{2}} [ |T\rangle_c |S\rangle_a |T\rangle_t - |T\rangle_c |T\rangle_a |S\rangle_t ] + \\
&\quad \frac{\alpha\delta}{\sqrt{2}} [ |T\rangle_c |S\rangle_a |S\rangle_t - |T\rangle_c |T\rangle_a |T\rangle_t ] + \\
&\quad \frac{\beta\gamma}{\sqrt{2}} [ |S\rangle_c |T\rangle_a |T\rangle_t - |S\rangle_c |S\rangle_a |S\rangle_t ] + \\
&\quad \frac{\beta\delta}{\sqrt{2}} [ |S\rangle_c |T\rangle_a |S\rangle_t - |S\rangle_c |S\rangle_a |T\rangle_t ]. \tag{B.30}
\end{aligned}$$

Measuring the ancilla in a singlet or triplet results in the final eight states:

$$\begin{aligned}
|\psi_{1,1,1}\rangle &= \alpha\gamma |T\rangle_c |S\rangle_t + \alpha\delta |T\rangle_c |T\rangle_t + \beta\gamma |S\rangle_c |T\rangle_t + \beta\delta |S\rangle_c |S\rangle_t, \tag{B.31} \\
|\psi_{1,1,0}\rangle &= \alpha\gamma |T\rangle_c |T\rangle_t + \alpha\delta |T\rangle_c |S\rangle_t + \beta\gamma |S\rangle_c |S\rangle_t + \beta\delta |S\rangle_c |T\rangle_t, \\
|\psi_{1,0,1}\rangle &= -\alpha\gamma |T\rangle_c |S\rangle_t - \alpha\delta |T\rangle_c |T\rangle_t + \beta\gamma |S\rangle_c |T\rangle_t + \beta\delta |S\rangle_c |S\rangle_t, \\
|\psi_{1,0,0}\rangle &= \alpha\gamma |T\rangle_c |T\rangle_t + \alpha\delta |T\rangle_c |S\rangle_t - \beta\gamma |S\rangle_c |S\rangle_t - \beta\delta |S\rangle_c |T\rangle_t, \\
|\psi_{0,1,1}\rangle &= \alpha\gamma |T\rangle_c |T\rangle_t + \alpha\delta |T\rangle_c |S\rangle_t + \beta\gamma |S\rangle_c |S\rangle_t + \beta\delta |S\rangle_c |T\rangle_t, \\
|\psi_{0,1,0}\rangle &= \alpha\gamma |T\rangle_c |S\rangle_t + \alpha\delta |T\rangle_c |T\rangle_t + \beta\gamma |S\rangle_c |T\rangle_t + \beta\delta |S\rangle_c |S\rangle_t, \\
|\psi_{0,0,1}\rangle &= \alpha\gamma |T\rangle_c |T\rangle_t + \alpha\delta |T\rangle_c |S\rangle_t - \beta\gamma |S\rangle_c |S\rangle_t - \beta\delta |S\rangle_c |T\rangle_t, \\
|\psi_{0,0,0}\rangle &= -\alpha\gamma |T\rangle_c |S\rangle_t - \alpha\delta |T\rangle_c |T\rangle_t + \beta\gamma |S\rangle_c |T\rangle_t + \beta\delta |S\rangle_c |S\rangle_t.
\end{aligned}$$

Applying the gates  $\sigma_c, \sigma_t$  on the control and target qubits in accordance to the results of the parity and ancilla measurements (as shown in appendix B.1) results in the same state in all eight computation branches (up to a global phase):

$$|\psi_f\rangle = \alpha\gamma |T\rangle_c |T\rangle_t + \alpha\delta |T\rangle_c |S\rangle_t + \beta\gamma |S\rangle_c |S\rangle_t + \beta\delta |S\rangle_c |T\rangle_t. \tag{B.32}$$

Under the computational interpretation this state is indeed the result of the CNOT gate:

$$f(|\psi_f\rangle) = \alpha\gamma |0\rangle_c |0\rangle_t + \alpha\delta |0\rangle_c |1\rangle_t + \beta\gamma |1\rangle_c |1\rangle_t + \beta\delta |1\rangle_c |0\rangle_t. \tag{B.33}$$

This proves the linearity of the gate.

## References

- [1] M. A. Nielsen and I. L. Chuang. *Quantum Computation and Quantum Information*. Press Syndicate of the University of Cambridge, Cambridge, 2000.
- [2] J. Levy. Universal quantum computation with spin-1/2 pairs and heisenberg exchange. *Phys. Rev. Lett.*, 89:147902, 2002.
- [3] L. A. Wu and D. A. Lidar. Power of anisotropic exchange interactions: Universality and efficient codes for quantum computing. *Phys. Rev. A*, 65:042318, 2002.
- [4] L. A. Wu and D. A. Lidar. Universal quantum logic from Zeeman and anisotropic exchange interactions. *Phys. Rev. A*, 66:062314, 2002.
- [5] M. S. Byrd and D. A. Lidar. Comprehensive encoding and decoupling solution to problems of decoherence and design in solid-state quantum computing. *Phys. Rev. Lett.*, 89:047901, 2002.
- [6] D. P. DiVincenzo, D. Bacon, J. Kempe G. Burkard, and K. B. Whaley. Universal quantum computation with the exchange interaction. *Nature*, 408:339, 2000.
- [7] J. Kyriakidis and S. J. Penney. Coherent rotations of a single spin-based qubit in a single quantum dot at fixed Zeeman energy. *Phys. Rev. B*, 71:125332, 2005.
- [8] F. Meier, J. Levy, and D. Loss. Quantum computing with spin cluster qubits. *Phys. Rev. Lett.*, 90:047901, 2003.
- [9] S. Bravyi. Universal quantum computation with the  $\nu = 5/2$  fractional quantum Hall state. *Phys. Rev. A*, 73(042313), 2006.
- [10] F. Wilczek. Magnetic flux and angular momentum, and statistics. *Phys. Rev. Lett.*, 48:1144–1146, 1982.
- [11] F. Wilczek. Quantum Mechanics of Fractional-Spin Particles. *Phys. Rev. Lett.*, 49:957–959, 1982.
- [12] F. Wilczek. Disassembling anyons. *Phys. Rev. Lett.*, 69:132–135, 1992.
- [13] J. Preskill. Lecture notes on quantum computation. <http://www.theory.caltech.edu/people/preskill/ph229/>, 1997.

## REFERENCES

---

- [14] A. Kitaev. Fault-tolerant quantum computation by anyons. *Ann. Phys.*, 303:2–30, 2003.
- [15] M. H. Freedman, A. Kitaev, M. J. Larsen, and Z. Wang. Topological quantum computation. *quant-ph*, page 0101025, 2002.
- [16] E. Dennis, A. Kitaev, A. Landahl, and J. Preskill. Topological quantum memory. *Math. Phys.*, 43:4452–4505, 2002.
- [17] R. Willett, J. P. Eisenstein, H. L. Störmer, D. C. Tsui, A. C. Gossard, and J. H. English. Observation of an even-denominator quantum number in the fractional quantum Hall effect. *Phys. Rev. Lett.*, 59:1776–1779, 1987.
- [18] G. Moore and N. Read. Nonabelions in the fractional quantum Hall effect. *Nucl. Phys. B*, 360:362–396, 1991.
- [19] C. Nayak and F. Wilczek.  $2n$  quasihole states realize  $2^{n-1}$  dimensional spinor braiding statistics in paired quantum Hall states. *Nucl. Phys. B*, 479(3):529–553, 1996.
- [20] D. Loss and D. P. DiVincenzo. Quantum computation with quantum dots. *Phys. Rev. A*, 57:120–126, 1998.
- [21] J. R. Petta, A. C. Johnson, J. M. Taylor, E. A. Laird, A. Yacoby, M. D. Lukin, C. M. Marcus, M. P. Hanson, and A. C. Gossard. Coherent manipulation of coupled electron spins in semiconductor quantum dots. *Science*, 309:2180–2184, 2005.
- [22] R. Hanson, L. H. Willems van Beveren, I. T. Vink, J. M. Elzerman, W. J. M. Naber, F. H. L. Koppens, L. P. Kouwenhoven, and L. M. K. Vandersypen. Single-shot readout of electron spin states in a quantum dot using spin-dependent tunnel rates. *Phys. Rev. Lett.*, 94:196802, 2005.
- [23] G. Nogues, A. Rauschenbeutel, S. Osnaghi, M. Brune, J.M. Raimond, and S. Haroche. Seeing a single photon without destroying it. *Nature*, 400:239, 1999.
- [24] E. Knill, R. Laflamme, and G. J. Milburn. A scheme for efficient quantum computation with linear optics. *Nature*, 409:46–52, 2001.
- [25] J. L. O’Brien, G. J. Pryde, A. G. White, T. C. Ralph, and D. Branning. Demonstration of an all-optical quantum controlled-not gate. *Nature*, 426:264–267, 2003.

## REFERENCES

---

- [26] H. A. Engel and D. Loss. Fermionic Bell-state analyzer for spin qubits. *Science*, 309:586–588, 2005.
- [27] C. W. J. Beenakker, D. P. DiVincenzo, C. Emary, and M. Kindermann. Charge detection enables free-electron quantum computation. *Phys. Rev. Lett.*, 93:020501, 2004.